

陸沿岸部震災被災地域との皮膚科遠隔診療の試み
 一陸前高田診療所（岩手県医師会）と岩手医科大学皮膚科との遠隔皮膚科診療—

赤坂 俊英 高橋 和宏

岩手医科大学皮膚科学講座

The trial of dermatological tele-medicine with Rikuzen-Takata clinic (Iwate medical association) in the Sanriku shore area where is the earthquake disaster stricken area and the dermatology of Iwate Medical University

Toshihide Akasaka Kazuhiro Takahashi

Iwate Medical University, School of Medicine

要旨

東日本大震災津波により壊滅的な被害を受けた陸前高田地域の皮膚科医は皆無となった。そこで、陸前高田診療所（岩手県医師会）と岩手医科大学皮膚科との遠隔皮膚科診療を試み、遠隔診療が医療過疎の解消の一助となるかを検討した。通信方法は専用回線を用い、診療現場に検査機器、ムービーカメラ、照明器具を用い、岩手医科大学には皮膚科専門医が待機するシステムを構築して行った。その結果、1) 遠隔医療機器システム立ち上げまでの時間は平均40分であった。2) 1人の患者に要する遠隔医療の時間は平均34分であった。患者への説明と同意取得、診断機器や映像機器の切り替えに時間を要した。3) 診断一致率は22例中21例が一致(95%)していた。診断確定に苦慮した例の多くは、①頭皮の毛髪間や指間、口腔内、陰部・腋窩部などの皮膚の焦点が合わない、②蕁麻疹など淡い紅斑の色調あるいは常色の軽い扁平な盛り上がりか画像で認識しがたい、③アナフィラキシー紫斑病など微小点状出血は映像では不明瞭である、④悪性黒色腫の初期病変や軽症の太田母斑の淡い黒色斑や青色斑は映像で不明瞭である、⑤真菌検査の菌糸の画像が不明瞭である、などであった。これらの問題は診断を補助する機器の充実で改善すると考えられた。4) 患者からの遠隔診療に対する評価はVASで66%であった。①大きなモニター画像に映し出され、おどろいた、②診察のスキミングが感じられない、③診察時間が長すぎる、④カメラに追い回されている感じがする、などの意見があった。しかし、意見の多くは専門医の診察・判断を仰ぐことができ、安心感を示すものが多くみられた。本研究によって、他科の医師と機器操作に熟練した技術者の存在のもとに皮膚科遠隔医療が可能であることが示唆された。しかし、緊急に改善すべき、①遠隔医療に関する受診者の理解、②通用性に優れたムービーカメラの精度向上、などの問題点が提起された。

キーワード：東日本大震災津波、陸前高田地域、皮膚科遠隔診療、高性能ムービーカメラ、NTT専用回線

1. はじめに

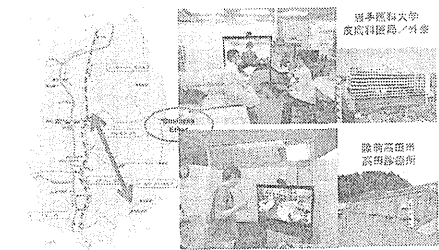
岩手県三陸沿岸地域は以前から医療過疎地域であった。皮膚科診療を有する総合病院が5カ所（うち皮膚科常勤医は1人）、皮膚科開業医診療所が3カ所と皮膚科領域についても医療過疎地域であった。東日本大震災津波により壊滅的な被害を受けた三陸沿岸地域、特に陸前高田地域では開業医1人によって皮膚科診療が行われていたが、震災に被災した都市に避難したため同地域には皮膚科医は皆無となった。一方、岩手医科大学附属病院は、「岩手県東日本大震災津波復興計画」のなかで、被災した医療過疎地

域に対して皮膚科領域も含め医療情報機器等を活用した遠隔医療によって高度な専門医療を提供する役割を求められている。

一方、従来の皮膚科遠隔医療は個別的な支援や単なる疾患の診断に留まっており、検査や診断・治療など総合的医療の提供はできていない。本研究では三陸沿岸部震災被災地域である陸前高田診療所（岩手県医師会）と岩手医科大学皮膚科との遠隔皮膚科診療を試み、遠隔診療が医療過疎の解消の一助となるかを検討した。

2. 目的

本研究では、①被災した医療過疎地域において災害拠点病院である大学病院が皮膚科遠隔医療によって高度医療を安定的に提供するための施設・設備・人員体制・コスト等についての検討と②対面診療と比較した遠隔医療の質についての検討を行う。①においては、専用回線を用い、診療現場に検査機器、ムービーカメラ、照明器具を用い、これらの器材の使用法に熟練した人材がいることであること、また、岩手医科大学には皮膚科専門医が2名待機するシステムを構築する。②においては、皮膚疾患患者を対象として、陸前高田診療所における皮膚科専門医による対面診療と遠隔診療とを比較検討する【図1】。



【図1】遠隔医療構築実証プロジェクト概要

3. 方法

1. 研究倫理および記録保存

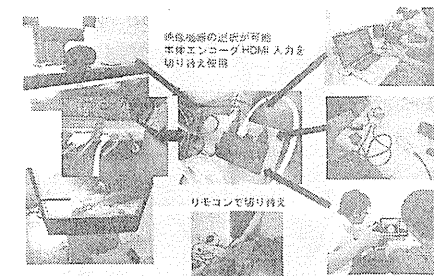
本研究は岩手医科大学倫理委員会の許可を得た。実験は患者のインフォームドコンセントを得て行う。患者情報や画像は匿名化し、個人を特定できないようにする。また、各患者の対面診療の動画は岩手医科大学情報センターにサーバー室を設けて保管した。医療情報は高田診療所の診療録に同診療所医師が記載し、同診療所に保管した。診療録の一部は患者および高田診療所の許可のもと、研究資料として用いた。

2. 利用回線および診療現場の器材

画像および医療情報の更新はNTT専用回線（NTT Business Ether）を使用した。実験に先駆けて、対面診療による問診のためにテレビ電話付き大型モニターを含むテレビ会議文信システム（フルHD（1080P/30fps））【図2】、患部の撮影のため2機の高性能ムービーカメラ、1機の複写カメラ、真菌検査および病理組織検査標本確認のためにオリンパス顕微鏡、患者情報記録のためノートパソコン、FAX機を配置した【図3】。それぞれを接続し、必要に応じてこれらの機器を切り替えて使用した。また、画像の色調を統一化、一定化するためにLED照明システムを使用した。これらのシステムで遠隔診断と医療提供が可能かを評価すると共にシステム設定にかかる時間も計測した。



【図2】高田診療所のシステム機器

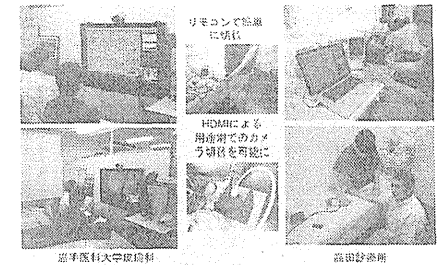


【図3】高田診療所カメラの切り替え状況

3. 遠隔対面診療の評価方法

研究の大半は高田診療所に皮膚科専門医が指向き、インフォームドコンセントの取得、患者の問診、診療録記載、処方箋発行、皮膚検査、機器の設定、皮膚病変の撮影、岩手医科大学皮膚科専門医との文信を行い、以下について評価した。平成25年1月末まで計22人の皮膚科患者の診療を行った【図4】。

- 1) 患者1人の診療時間
- 2) 診断名：高田診療所と岩手医科大学の皮膚科専門医の



【図4】皮膚科患者画像の送受態状況

- 診断の一致率
- 3) 皮膚の部位で診断しにくい部位
 - 4) 皮膚の形態で診断しにくい皮膚
 - 5) 患者満足度（通常の対面診療と比較したVASで表示：100%が通常対面診療と同等、0%が全く対面診療に値しない）

4. 結果

- 1) 診療前の遠隔医療機器システム立ち上げまでにかかる時間は平均40分であった。熟練すると短縮可能と考えられた。
- 2) 1人の患者に要する遠隔医療の時間は最短26分、最長52分、平均34分であった。患者への説明と同意取得、診断機器や映像機器の切り替えに時間を要した。
- 3) 診断一致率は22例中21例が一致(95%)していた。診断確定に苦慮した例の多くは、①頭皮の毛髪間や指間、口腔内、陰部・腋窩部などの皮膚の映像の焦点が合わない、②蕁麻疹など淡い紅斑の色調あるいは常色の軽い扁平な盛り上がりか画像で認識しがたい、③アナフィラキシー紫斑病など微小点状出血は映像では不明瞭である、④悪性黒色腫の初期病変や軽症の太田母斑の淡い黒色斑や青色斑は映像で不明瞭である、⑤真菌検査の菌糸の画像が不明瞭である、などによるものであった。これらの問題は診断を補助する機器の充実で改善すると考えられた。
- 4) 患者からの遠隔診療に対する評価はVisual Analog Scale (VAS) で66%であった。①大きなモニター画像に映し出され、おどろいた、②診察のスキミングが感じられない、③診察時間が長すぎる、④カメラに追い回されている感じがする、などの意見があった。しかし、意見の多くは専門医の診察・判断を仰ぐことができ、安心感を示すものが多くみられた。

5. 考察

本研究の最終目標は遠隔地に皮膚科専門医がいない状況での遠隔診療である。他科の医師と機器操作に熟練した技術者の存在のもとに皮膚科遠隔医療が可能であることが示唆された。①遠隔医療に関する受診者の理解、②他科の医師の皮膚科遠隔医療に対する理解、③カメラ、検査機器、コンピュータの操作に熟練した技術者の存在、④患者誘導や発疹の遷移に熟練した看護師の存在、⑤通用性に優れたムービーカメラの精度向上、⑥診断精度向上のための機器（皮膚温検査機、エコー機器など）の必要性、⑦画像および遠隔診療カルテの保存方法の改善、⑧診療費用の配分。

References

- Walsh NM, Murray S, D'Intino Y. Eruptive xanthomata with urate-like crystals. *J Cutan Pathol* 1994; 21: 350-355.
- Bito T, Kawakami C, Shimajiri S, Tokura Y. Generalized eruptive xanthoma with prominent deposition of naked chylomicrons: evidence for chylomicrons as the origin of urate-like crystals. *J Cutan Pathol* 2010; 37: 1161-1163.

- Kodama H, Akiyama H, Nagao Y, et al. Persistence of foam cells in rabbit xanthoma after normalization of serum cholesterol level. *Arch Dermatol Res* 1988; 280: 108-113.
- Bergman R, Aviram M, Shemer A, et al. Enhanced low-density lipoprotein degradation and cholesterol synthesis in monocyte-derived macrophages of patients with adult xanthogranulomatosis. *J Invest Dermatol* 1993; 101: 880-882.

Annular elastolytic giant cell granuloma developing on lesions of vitiligo

Dear Editor,

A 74-year-old woman presented with a two-year history of reddish annular nodules on the neck, trunk, and forearms. She had a 10-year history of generalized vitiligo that had been untreated. The nodules with elevated borders and central atrophy and hypopigmentation, 0.5-1 cm in diameter, were located on the neck, trunk, and forearms (Fig. 1). These nodules had developed mainly on the preexisting vitiligo lesions. The patient had been taking bendipine hydrochloride for hypertension for the last 14 years. She had no history of diabetes mellitus or sarcoidosis.

A skin biopsy was taken from a nodule on the forearm. Hematoxylin and eosin staining of the specimen showed a granulomatous infiltrate of lymphocytes, histiocytes,

and multinucleated giant cells in the upper and middle dermis without palisading (Fig. 2a). Immunohistochemistry showed that the lymphocytes in the inflammatory infiltrate were positive for CD3, CD4⁺ T-cells predominated over CD8⁺ T-cells, and the histiocytes and multinucleated giant cells were positive for CD68. Almost all of the epidermal cells were negative for Melan-A (Fig. 2b). Slight mucin deposition was evident. Elastic van Gieson staining showed that elastic fibers were absent from the reticular dermis in the area surrounded by the granulomatous infiltrate (Fig. 2c). Fragmented elastic fibers were present within some of the histiocytes and multinucleated giant cells (Fig. 2d). Ziehl-Neelsen and PAS staining revealed no acid-fast bacilli or fungal organisms. Laboratory examinations, including a full blood cell count, routine biochemistry, fasting blood sugar level, and urinalysis gave normal results. These findings were consistent with

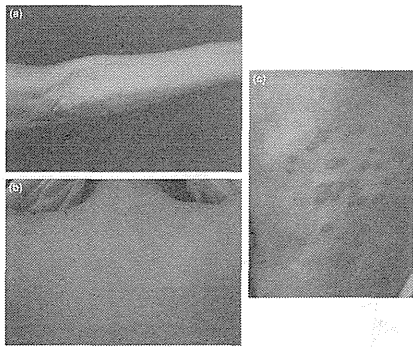


Figure 1 Multiple, erythematous, marginally elevated, annular nodules and round papules, developed mainly on lesions of preexisting vitiligo, distributed on the back (a), forearms (b) and abdomen (c)

International Journal of Dermatology 2013, 52, 1338-1461

© 2012 The International Society of Dermatology

© 2012 The International Society of Dermatology

International Journal of Dermatology 2013, 52, 1338-1461

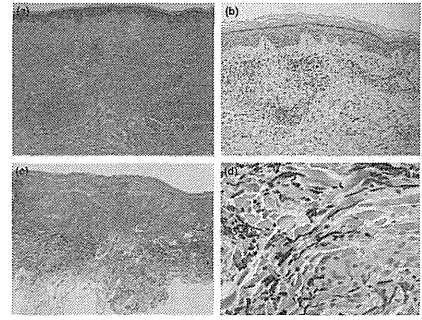


Figure 2 (a) Granulomatous infiltrates of lymphocytes, histiocytes and multinucleated giant cells in the upper and middle dermis without palisading (hematoxylin and eosin, original magnification $\times 40$). (b) Almost all of the epidermal cells were negative for Melan-A (original magnification $\times 100$). (c) Elastic van Gieson staining demonstrates the absence of elastic fibers in the reticular dermis in the area surrounded by the granulomatous infiltrate (original magnification $\times 40$). (d) Fragmented elastic fibers are present within some of the histiocytes and multinucleated giant cells (original magnification $\times 400$)

annular elastolytic giant cell granuloma (AEGCG). Thereafter, the patient was treated with topical corticosteroid (clobetasol propionate). This resulted in gradual flattening of the nodules, some of which finally disappeared.

Annular elastolytic giant cell granuloma is an entity that was proposed originally by Hanke *et al.*¹ for cutaneous annular lesions characterized by elastolysis, elastophagocytosis, and an infiltrate of multinucleated giant cells. The pathogenesis of AEGCG remains unclear. It has been postulated that exposure to the sun or other unknown factors alters the antigenicity of the elastic fibers and induces cell-mediated immune reactions.²

Interestingly, in the present case, AEGCG occurred mainly on pre-existing lesions of vitiligo. This anatomical co-localization suggests that the association between the two disorders is not accidental. The pathogenesis of vitiligo is also still unknown, although recently it has been shown that oxidative stress and accumulation of free radicals (FRs) acting as a trigger of melanocyte degeneration in the epidermis of affected skin are involved.³ Oxidative stress can be induced by an increase in the generation of reactive oxygen species (ROS) and other radicals. Recent studies of vitiligo have shown that FRs are increased and that antioxidant systems are deficient. It has been demonstrated both *in vivo* and *in vitro* that patients with vitiligo accumulate high levels of hydrogen peroxide (H_2O_2), which

leads to the destruction of melanocytes in the epidermis.⁴ On the other hand, high superoxide dismutase activity in the serum and skin of patients with stable vitiligo has been reported.^{5,6} These changes would lead to the accumulation of H_2O_2 .

Recent studies of photoaging have revealed that ultraviolet (UV) irradiation induces the formation of ROS in skin tissue. Dermal fibroblasts exposed to ROS show increased expression of mRNA for matrix metalloproteinases (MMP)-1 and MMP-2, which have the ability to degrade collagen and elastic fibers.^{7,8} Igawa *et al.*⁹ have reported that oral Dapsone, which has an anti-oxidative effect, is effective for treatment of AEGCG. In our present patient, annular nodules were located on covered, as well as sun-exposed areas, and the patient had not been treated with UV irradiation. We postulate that in this case, degradation of dermal elastic fibers in the vitiligo lesions may have triggered the accumulation of lymphocytes and macrophages, elastophagocytosis, and subsequent granuloma formation.

Daisuke Watabe, MD
Toshibide Akasaka, MD

From the Department of Dermatology
Iwate Medical University School of Medicine
Morioka
Japan

Correspondence

Daisuke Watabe, MD

Department of Dermatology
Iwate Medical University School of Medicine

19-1 Uchimarui

Morioka 020-8505

Japan

E-mail: dwatabe@iwate-med.ac.jp

Conflicts of interest: None declared.

References

- Hanke CW, Batlin PL, Roenigk JH Jr. Annular elastolytic giant cell granuloma. A clinicopathologic study of five cases and a review of similar entities. *J Am Acad Dermatol* 1979; 11: 412-421.
- Okaya-Bayazit E, Bayuklbahani N, Baykal C, et al. Annular elastolytic giant cell granuloma: sparing of a burn scar and successful treatment with chloroquine. *Br J Dermatol* 1999; 140: 525-530.
- Dell'ana ML, Picardo M. A review and a new hypothesis for non-immunological pathogenetic mechanisms in vitiligo. *Pigment Cell Res* 2006; 19: 406-411.

Spiny keratoderma of the palms in an insulin-treated diabetic patient

Spiny keratoderma is a rare disease characterized by multiple discrete keratotic plugs, resembling a "music box spine", arising from the palms, soles, or both.¹ It was first described in 1971 by Brown², who called it punctate keratoderma. These spiny lesions have been described as filiform hyperkeratosis,³ minute digitate hyperkeratosis,⁴ punctate keratoderma,⁵ punctate parakeratotic keratoderma⁶ and, most recently, spiny keratoderma of the palms and soles.⁷ Most of the cases described represent acquired disease, but there are also familial cases. Associations with a systemic disease or malignancy occur in some acquired cases. We present the case of a man with acquired spiny keratoderma who was receiving insulin treatment for type 2 diabetes mellitus.

A 58-year-old Japanese male was referred to us because of multiple asymptomatic, keratotic papules on his fingers and palms. He had a more than 20-year history of diabetes mellitus. He had noted the lesions more than 10 years ago and had started insulin treatment around the same time. Family history was negative for keratoderma, ichthyosis, or other dermatological diseases. He had no history of renal failure or hyperlipidemia and was unaware of any arsenic exposure.

On physical examination, numerous firm keratotic spicules were seen on the volar surface of the palms and

- Schallreuter KU, Moore J, Wood JM, et al. *In vivo* and *in vitro* evidence for hydrogen peroxide (H_2O_2) accumulation in the epidermis of patients with vitiligo and its successful removal by a UVB-activated pseudocatalase. *J Invest Dermatol Symp Proc* 1999; 4: 91-96.
- Ines D, Sonia B, Riadh BM, et al. A comparative study of oxidant-antioxidant status in stable and active vitiligo patients. *Arch Dermatol Res* 2006; 298: 147-152.
- Yildirim M, Baysal V, Inaloz HS, Can M. The role of oxidants and antioxidants in generalized vitiligo at tissue level. *J Eur Acad Dermatol Venereol* 2004; 18: 683-686.
- Kawaguchi Y, Tanaka H, Okada T, et al. The effects of ultraviolet A and reactive oxygen species on the mRNA expression of 72-kDa type IV collagenase and its tissue inhibitor in cultured human dermal fibroblasts. *Arch Dermatol Res* 1996; 288: 39-44.
- Zaw KK, Yokoyama Y, Abe M, Ishikawa O. Catalase restores the altered mRNA expression of collagen and matrix metalloproteinases by dermal fibroblasts exposed to reactive oxygen species. *Eur J Dermatol* 2006; 16: 375-379.
- Igawa K, Maruyama R, Katayama I, Nishioka K. Anti-oxidative therapy with oral dapsone improved HCV antibody-positive annular elastolytic giant cell granuloma. *J Dermatol* 1997; 24: 328-331.

fingers (Fig. 1). The lesions were 0.5-1 mm in diameter, 1-2 mm in length, and skin-colored. There were no similar lesions at other sites, including the soles.

Histopathological examination of skin biopsy specimens of the palms showed large columns of keratin arising from the epidermis in an area with a focally decreased granular layer and parakeratosis (Fig. 2). No dyskeratotic or vacuolated keratinocytes were seen in the underlying epidermis. Blood tests and computer tomography scan showed no abnormalities. Results of upper and lower endoscopy did not reveal any malignant neoplasms.

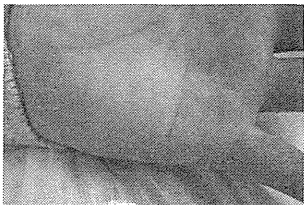


Figure 1 Multiple yellowish filiform keratotic projections on the left palm

International Journal of Dermatology 2013, 52, 1338-1461

© 2013 The International Society of Dermatology

Case Study

Subcutaneous Panniculitis-Like T-Cell Lymphoma (SPTCL) with Hemophagocytosis (HPS): Successful Treatment Using High-Dose Chemotherapy (BFM-NHL & ALL-90) and Autologous Peripheral Blood Stem Cell Transplantation

Eiichi Sakurai,^{1,2)} Takashi Satoh,³⁾ Yashima-Abo Akiko,³⁾ Chihaya Maesawa,³⁾
Kanako Tsunoda,^{1,2)} Mikiya Endo,³⁾ Toshihide Akasaka,¹⁾ and Tomoyuki Masuda³⁾

Subcutaneous panniculitis-like T-cell lymphoma (SPTCL) is a rare form of non-Hodgkin lymphoma, in which lymphoma cells infiltrate preferentially into subcutaneous adipose tissue. Although various treatment trials for SPTCL have been attempted, no standardized therapy has been established. Here, we report a case of $\alpha\beta^+$ T-cell-phenotype SPTCL (SPTCL-AB) with hemophagocytosis (HPS) in a 14-year-old girl, who presented with low-grade fever, general fatigue and chest swelling. Laboratory examinations revealed leukocytopenia, and bone marrow aspiration cytology showed HPS. The diagnosis of SPTCL-AB was made by biopsy on the basis of thickened subcutaneous tissue in the chest wall. Following high-dose chemotherapy (HDT) of BFM-NHL & ALL-90, autologous peripheral blood stem cell transplantation (auto-PBSCT) was performed. The patient responded to the treatment and has remained asymptomatic for 2 years. Our results suggest that a combination of HDT of BFM-NHL & ALL-90 and auto-SCT treatment is effective for SPTCL associated with HPS. [*J Clin Exp Hematop* 53(2): 135-140, 2013]

Keywords: SPTCL, hemophagocytosis, BFM-NHL & ALL-90, auto-PBSCT

INTRODUCTION

In 1991, the distinct clinicopathological features of a T-cell lymphoma in which the lymphoma cells preferentially invade the subcutaneous tissue were described by Gonzalez *et al.*¹ Under the term subcutaneous panniculitis-like T-cell lymphoma (SPTCL), this new condition was established as a distinct disease entity in the World Health Organization (WHO) classification.² Because of its peculiar pathological features, SPTCL may be initially misdiagnosed as Weber-Christian disease, a benign inflammatory panniculitis and a granulomatous disease.^{3,4} Recent studies have disclosed that cases with an $\alpha\beta^+$ T-cell phenotype (SPTCL-AB) and a $\gamma\delta^+$ T-cell phenotype (SPTCL-GD) can be distinguished within

the group of SPTCL.⁵ SPTCL-ABs have a CD4⁺, CD8⁻, CD56⁻ phenotype, and SPTCL-GDs have a CD4⁺, CD8⁻ phenotype with frequent expression of CD56. Compared with SPTCL-ABs, SPTCL-GDs have a poor prognosis.^{6,7} On the basis of these observations, the term SPTCL is used only for SPTCL-ABs, and SPTCL-GDs are included within the cutaneous $\gamma\delta^+$ T-cell lymphomas.^{8,9} Although SPTCL-AB patients without hemophagocytic syndrome (HPS) have a favorable prognosis, the clinical course of cases associated with HPS is generally aggressive, and a delay in diagnosis or treatment may result in a fatal outcome. There have been few reports of successful treatment of SPTCL-AB patients with HPS, and no therapeutic regimen has been established. Here, we report a case of SPTCL-AB with HPS that was treated successfully with a combination of high-dose chemotherapy (HDT) of Berlin-Frankfurt-Münster-non-Hodgkin lymphoma-90 (BFM-NHL-90) and autologous peripheral blood stem cell transplantation (auto-PBSCT).

CASE REPORT

A previously healthy 14-year-old Japanese girl visited a physician because of a 1-month history of chest swelling.

Sakurai E, *et al.*

She also had a 3-month history of general fatigue and low-grade fever. Initial laboratory examinations revealed a white blood cell count of $2.82 \times 10^3/\mu\text{L}$, hemoglobin of 11.6 g/dL, hematocrit of 33.8 g/dL, and platelet count of $16.4 \times 10^3/\mu\text{L}$. Histopathologic examination of a biopsy specimen of subcutaneous adipose tissue from the chest wall revealed diffuse infiltration of medium-sized lymphocytes. Under a diagnosis of panniculitis due to lupus profundus, administration of low-dose prednisolone (PSL) was started. Several weeks later, the chest swelling expanded gradually. She was therefore referred and admitted to our hospital for further evaluation and treatment.

On physical examination, a massive tumor was evident in her chest subcutaneous tissue (Fig. 1). The findings from laboratory examinations were as follows: aspartate aminotransferase 27 IU/L (normal: 10-40 IU/L), alanine aminotransferase 15 IU/L (normal: 5-35 IU/L), lactate dehydrogenase 235 U/L (normal: 115-359 IU/L), soluble interleukin-2 receptor 641 U/mL (normal: 220-530 U/mL) and ferritin 56 ng/mL. Moreover, previous infection with Epstein-Barr virus was evident. Magnetic resonance imaging revealed noticeable thickening of the subcutaneous tissue, compatible with the region of the massive tumor in the chest (Fig. 2). Histopathology of skin biopsy specimens showed medium-sized lymphocytes diffusely infiltrating into the subcutaneous fat tissue (Fig. 3a). Rimming of the lymphocytes around individual fat cells was observed (Fig. 3b).

Immunohistochemical staining revealed that the infiltrating lymphocytes were CD3⁺, CD4⁺, CD5⁺, CD8⁺, CD20⁺, CD30⁺, CD45RO⁺, CD56⁻ and CD79a⁺ (Fig. 4). They were positive for T-cell receptor- β (Fig. 5a). Cytotoxic molecules such as granzyme B, T-cell intracellular antigen-1 (TIA-1) and perforin were positive (Fig. 5b). Latent membrane protein 1 (LMP-1) and EBV *in situ* hybridization were negative (Fig. 5c & 5d). Bone marrow smears showed hemophagocytosis.

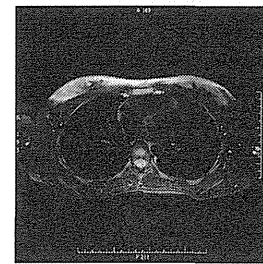


Fig. 2. Magnetic resonance imaging of the chest (T2-weighted). The subcutaneous tumor of the chest wall showed high signal intensity.

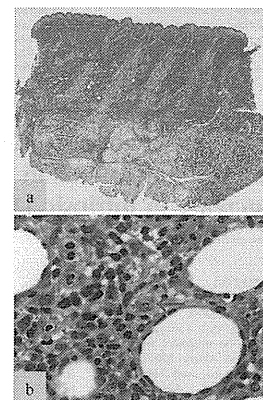


Fig. 3. Histopathology of the skin biopsy specimen (H&E stain). (3a) Diffuse cellular infiltration occurred in the subcutaneous fat tissue. (3b) Rimming of lymphocytes around fat cells was observed (arrows). Bean bag cells, phagocytosing erythrocytes, were found among the lymphocytes. (3a) $\times 10$, (3b) $\times 400$.

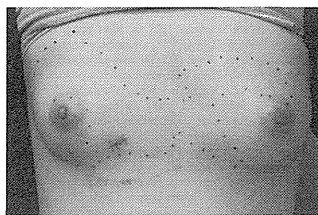


Fig. 1. A massive tumor, indicated by black dots, was present in the subcutaneous tissue of the chest.

Received: January 4, 2013

Revised: March 12, 2013

Accepted: April 11, 2013

Departments of Dermatology, Pathology and Pediatrics, School of Medicine, Iwate Medical University, Morioka, Japan

Corresponding author: Eiichi Sakurai, MD, Departments of Dermatology and Pathology, School of Medicine, Iwate Medical University, Uchimaru 19-1, Morioka 020-8505, Japan

e-mail: sakurai@iwate-med.ac.jp

135

136

SPTCL with hemophagocytosis

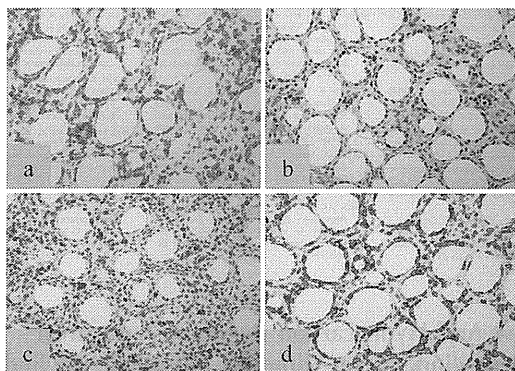


Fig. 4. Immunohistochemistry of CD3 (4a), CD4 (4b), CD5 (4c) and CD8 (4d). The infiltrating lymphocytes were positive for CD3, CD5 and CD8, but negative for CD4. $\times 400$.

DISCUSSION

SPTCL is a type of skin lymphoma characterized by the infiltration of subcutaneous tissue by pleomorphic T cells and benign macrophages, mimicking lobular panniculitis. This malignancy typically presents in the form of skin nodules that involve the extremities and can become ulcerated.⁹ The clinical course associated with HPS is aggressive, and a delay in diagnosis and treatment may result in a fatal outcome.

Although the mechanism of HPS in SPTCL has not been clarified, the phenomenon of HPS results from overproduction of cytokines, including interferon- γ , interleukin-2 (IL-2), IL-6, IL-12, IL-18 and tumor necrosis factor- α , produced by activated T cells (Th1 cells) and macrophages, which leads to a chain reaction of cytokines.¹⁰⁻¹³ Control of HPS in SPTCL-AB patients improves the prognosis.

Various therapies such as radiotherapy, PSL, CHOP (cyclophosphamide, hydroxydaunorubicin, vincristine and prednisolone) (like) chemotherapy and auto/allo-SCT have been applied for SPTCL-AB.⁹ For relapsed or refractory disease, various regimens have been attempted as salvage chemotherapy, including cladribine, DHAP (dexamethasone, cytarabine and cisplatin), ESHAP (etoposide, methylprednisolone, cytarabine and cisplatin), FLAG (fludarabine, cytarabine and granulocyte-colony stimulating factor), mini-BEAM (carmu-

Sakurai E, *et al.*

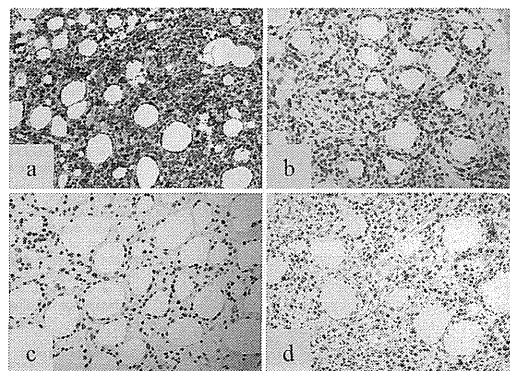


Fig. 5. Immunohistochemistry for T-cell receptor (TCR)- β (5a), granzyme B (5b), latent membrane protein-1 (LMP-1, 5c) and Epstein-Barr virus (EBV)-encoded RNA *in situ* hybridization (5d). Lymphocytes were positive for TCR- β , and expression of the cytotoxic molecule granzyme B was also found. LMP-1 and EBV were negative. $\times 200$.

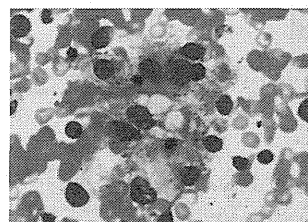


Fig. 6. Hemophagocytosis was seen in a smear of the bone marrow. Giemsa stain, $\times 1000$.

line, etoposide, cytarabine and melphalan) and VEPPB (vincristine, etoposide, prednisone, pobarbazine and bleomycin).⁹ However, no standardized treatment has yet emerged. In SPTCL-AB patients with HPS, a recent report has indicated that CHOP (like) chemotherapy is not very effective. Auto-SCT or allo-SCT following HDT has been suggested as an

important option for patients with refractory or recurrent SPTCL.^{4,14}

In the present case, high-dose PSL was initially used, but no response was obtained. Therefore, we treated the patient according to the BFM-NHL & ALL-90 protocol.

BFM-NHL-90 is a protocol for pediatric malignant lymphoma and yields a significantly better outcome for non-Hodgkin lymphoma at stage I or II.¹⁵ BFM-NHL-90 is also effective for pediatric anaplastic large-cell lymphoma. BFM-ALL-90 is a superior regimen for high-risk childhood T-cell acute lymphoblastic leukemia.¹⁶

The present case was treated successfully with a combination of HDT of BFM-NHL & ALL-90 followed by auto-PBSCT, and achieved clinical complete remission (CR). This result suggests that the BFM protocol is applicable and can yield complete remission in cases of SPTCL with HPS. Medhi *et al.* have also reported the value of the BFM-90 protocol for the treatment of patients with SPTCL and HPS.¹⁷

To date, there have been few reports of effective treatment for SPTCL using HDT following SCT. In almost all of the reported cases, the patients underwent HDT-allo-SCT and its effectiveness was impressive, 92% achieving CR, with a median response duration of ≥ 14 months.⁹ In intermediate- and high-grade lymphomas, myeloablative allo-SCT is associated

tosis of red blood cells and neutrophils by histiocytes (Fig. 6).

On the basis of these results, the patient was diagnosed as having SPTCL accompanied by HPS in spite of the low levels of lactate dehydrogenase and ferritin, and was treated with high-dose PSL (75 mg/day internally), starting on day 9 of admission.

Nine days later (on day 17 of admission), despite the PSL therapy, the chest tumor was unchanged in size. Additional HDT of BFM-NHL-90 (protocol I) was therefore applied. After starting the first course of the chemotherapy, the tumor in the chest gradually decreased in size. During the phase of recovery from the chemotherapy, peripheral blood stem cells (CD34⁺ cells) were harvested. Moreover, chemotherapy of BFM-NHL-90 (Protocol M) was applied as a consolidation therapy. In addition, one course of the BFM-acute lymphoblastic leukemia (ALL)-90 regimen (HR3) was applied for further treatment.

Following pretreatment with the MCVAC (ranimustine, cytarabine, etoposide and cyclophosphamide) regimen, the patient was treated with auto-PBSCT. The clinical course thereafter was uneventful. She has been in complete remission for more than 2 years, and there was no evidence of local recurrence in the chest wall and HPS in the bone marrow at the final follow-up examination.

137

138

with a lower relapse rate than auto-SCT for the graft-versus-leukemia effect.^{18,19} However, chronic graft-versus-host disease (cGVHD) is a very common complication, with a reported incidence of between 40% and 70%,²⁰ and is the leading cause of late death in allo-SCT survivors.^{20,21}

The median age of patients with SPTCL-AB at diagnosis is 36 years (range: 9-79 years), and about 19% are in the second decade or younger.² In children, cGVHD may reduce the quality of life because of the induction of growth irregularity. Mukai *et al.* described a patient with SPTCL and HPS who received HDT of BFM-NHL & ALL-90 and auto-SCT.⁴ The present case received a combination of HDT of BFM-NHL & ALL-90 and auto-SCT, and has been in complete remission for more than 2 years. This suggests that auto-SCT might be a feasible option following HDT.

In summary, we have reported a case of SPTCL complicated by HPS, which responded to treatment with HDT of BFM-NHL & ALL-90 and auto-SCT. Although the value of the BFM-NHL & ALL-90 protocol has to be further evaluated in SPTCL cases, our findings suggest that a combination of HDT of BFM-NHL & ALL-90 and auto-SCT is applicable for the treatment of SPTCL with HPS.

ACKNOWLEDGEMENTS

The authors express their thanks to Prof. Shigeo Nakamura, Nagoya University, Nagoya, Japan, for his advice.

DISCLOSURE/CONFLICT OF INTEREST

The authors state that they have no financial interest in the products mentioned within this article.

REFERENCES

- 1 Gonzalez CL, Medeiros LJ, Brazier RM, Jaffe ES: T-cell lymphoma involving subcutaneous tissue. A clinicopathologic entity commonly associated with hemophagocytic syndrome. *Am J Surg Pathol* 15:17-27, 1991
- 2 Jaffe ES, Gauri P, Raffinier E, Cerroni L, Meijer CJLM: Subcutaneous panniculitis-like T-cell lymphoma. In: Swerdlow SH, Campo E, Harris NL, Jaffe ES, Pileri SA, *et al.* (eds): *World Health Organization Classification of Tumours. WHO Classification of Tumours of Haematopoietic and Lymphoid Tissues*. 4th ed, Lyon, International Agency for Research on Cancer (IARC), pp.294-295, 2008
- 3 Tsukamoto Y, Katsunobu Y, Omura Y, Maeda I, Hirai M, *et al.*: Subcutaneous panniculitis-like T-cell lymphoma: successful initial treatment with prednisolone and cyclosporin A. *Intern Med* 45:21-24, 2006
- 4 Mukai HY, Okoshi Y, Shimizu S, Katsura Y, Takei N, *et al.*: Successful treatment of a patient with subcutaneous panniculitis-like T-cell lymphoma with high-dose chemotherapy and total body

irradiation. *Eur J Haematol* 70:413-416, 2003

- 5 Willemze R, Jaffe ES, Burg G, Cerroni L, Berti E, *et al.*: WHO-EORTC classification for cutaneous lymphomas. *Blood* 105:3768-3785, 2005
- 6 Massone C, Chott A, Metz D, Kerl K, Citarella L, *et al.*: Subcutaneous, blastic natural killer (NK), NK/T-cell, and other cytotoxic lymphomas of the skin: a morphologic, immunophenotypic, and molecular study of 50 patients. *Am J Surg Pathol* 28:719-735, 2004
- 7 Massone C, Lozzi GP, Egberts F, Fink-Puches R, Cota C, *et al.*: The protean spectrum of non-Hodgkin lymphomas with prominent involvement of subcutaneous fat. *J Cutan Pathol* 33:418-425, 2006
- 8 Willemze R, Jansen PM, Cerroni L, Berti E, Santucci M, *et al.*: Subcutaneous panniculitis-like T-cell lymphoma: definition, classification, and prognostic factors: an EORTC Cutaneous Lymphoma Group Study of 83 cases. *Blood* 111:838-845, 2008
- 9 Go RS, Wester SM: Immunophenotypic and molecular features, clinical outcomes, treatments, and prognostic factors associated with subcutaneous panniculitis-like T-cell lymphoma: a systematic analysis of 156 patients reported in the literature. *Cancer* 101:1404-1413, 2004
- 10 Imashuku S: Advances in the management of hemophagocytic lymphohistiocytosis. *Int J Hematol* 72:1-11, 2000
- 11 Akashi K, Hayashi S, Gondo H, Mizuno S, Harada M, *et al.*: Involvement of interferon- γ and macrophage colony-stimulating factor in pathogenesis of hemophagocytic lymphohistiocytosis in adults. *Br J Haematol* 87:243-250, 1994
- 12 Osugi Y, Hara J, Tagawa S, Takai K, Hosoi G, *et al.*: Cytokine production regulating Th1 and Th2 cytokines in hemophagocytic lymphohistiocytosis. *Blood* 89:4100-4103, 1997
- 13 Aricó M, Damesino C, Pende D, Moretta L: Pathogenesis of hemophagocytic lymphohistiocytosis. *Br J Haematol* 114:761-769, 2001
- 14 Alaiabac M, Berti E, Pigozzi B, Chiarion V, Aversa S, *et al.*: High-dose chemotherapy with autologous blood stem cell transplantation for aggressive subcutaneous panniculitis-like T-cell lymphoma. *J Am Acad Dermatol* 52 (Suppl):121-123, 2005
- 15 Kavan P, Kabicková E, Gajdos P, Koutocký J, Smelhaus V, *et al.*: Treatment of children and adolescents with non-Hodgkin's lymphoma (results based on the NHL Berlin-Frankfurt-Münster 90 protocol). *Cas Lek Cesk* 138:40-46, 1999
- 16 Schrauder A, Reiter A, Gädner H, Niehämmer D, Klingebiel T, *et al.*: Superiority of allogeneic hematopoietic stem-cell transplantation compared with chemotherapy alone in high-risk childhood T-cell acute lymphoblastic leukemia: results from ALL-BFM 90 and 95. *J Clin Oncol* 24:5742-5749, 2006
- 17 Medhi K, Kumar R, Rishi A, Kumar L, Bakshi S: Subcutaneous panniculitis-like T-cell lymphoma with hemophagocytosis: complete remission with BFM-90 protocol. *J Pediatr Hematol Oncol* 30:558-561, 2008
- 18 Ratanabharathorn V, Uberti J, Karanes C, Abella E, Lum LG: Prospective comparative trial of autologous versus allogeneic bone marrow transplantation in patients with non-Hodgkin's lymphoma.

Blood 84:1050-1055, 1994

- 19 Jones RJ, Ambinder RF, Piantadosi S, Santos GW: Evidence of a graft-versus-lymphoma effect associated with allogeneic bone marrow transplantation. *Blood* 77:649-653, 1991
- 20 Lee SJ, Klein JP, Barrett AJ, Ringden O, Antin JH, *et al.*: Severity of chronic graft-versus-host disease: association with

treatment-related mortality and relapse. *Blood* 100:406-414, 2002

- 21 Socié G, Stone JV, Wingard JR, Weisdorf D, Henslee-Downey PJ, *et al.*: Long-term survival and late deaths after allogeneic bone marrow transplantation. Late Effects Working Committee of the International Bone Marrow Transplant Registry. *N Engl J Med* 341:14-21, 1999

SHORT COMMUNICATION

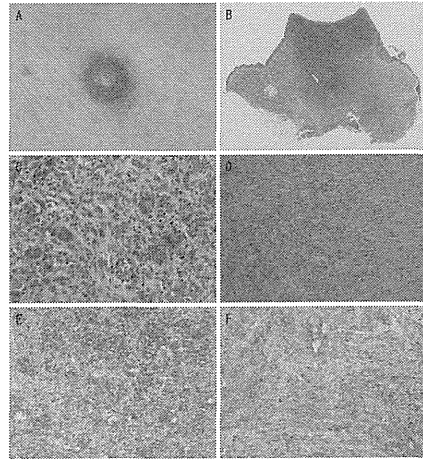
A Case of Atypical Fibrous Histiocytoma with Positivity for CD163 and CD44

Kansko Tsunoda¹, Kazuhiro Takahashi¹, Fumihiko Maeda¹, Hiroki Oikawa² and Toshihide Akasaka¹¹Departments of Dermatology and Pathology, School of Medicine, Iwate Medical University, Uchimaru 19-1, Morioka 020-8505, Japan. E-mail: tkansko@iwate-med.ac.jp

Accepted Dec 3, 2012; Epub ahead of print Mar 5, 2013

Atypical fibrous histiocytoma (AFH) is a variant of dermatofibroma (DF) that was first described by Fukamizu et al. (1) in 1983. Histologically AFH is characterized by proliferation of dermal spindle cells composed mainly of atypical histiocytic cells with striking nuclear pleomorphism and atypia, in a background of classic fibrous histiocytoma (2). It is known that many cases of AFH follow a benign course if complete excision is carried out (2, 3). However, because the tumour cells are atypical, AFH must be differentiated from tumours of intermediate malignancy, such as dermatofibrosarcoma protuberans (DFSP) or atypical fibrous xanthoma (AFX), as well as more malignant tumours, such as pleomorphic dermal sarcoma (PDS)/malignant fibrous histiocytoma (MFH).

We report here a case of AFH on the left upper arm of a 63-year-old woman and describe its immunoreactivity in detail. We also discuss the points of histological and immunohistological differentiation between AFH and other cutaneous spindle cell tumours.



CASE REPORT

A 63-year-old woman presented with an 8-month history of a symptomless, slowly growing swelling on the left upper arm. The patient had no unusual medical or family history. Clinical examination revealed an 8-mm black-purple hard mass with peripheral erythema (Fig. 1A). The tumour had arisen at a site without any known previous history of injury. A haemangioma was clinically suspected, and surgical excision was performed. Microscopic examination revealed a well-defined lesion, located in the dermis and extending to the subcutaneous tissue, with epidermal hyperplasia and a grenz zone (Fig. 1B). The lesion was composed largely of interlacing fascicles of predominant histiocyte-like eosinophilic spindle cells with elongated or plump vesicular nuclei, arranged in a storiform pattern. Abundant pleomorphic giant cells with huge bizarre nuclei (bi-lobed and multi-lobed) and histiocytes with large vesicular nuclei and prominent eosinophilic nucleoli were observed (Fig. 1C). In the peripheral region of the tumour, fibroblast-like spindle cells arranged in a storiform or fascicular pattern with collagen bundles were observed, resembling the classic features of DF. No necrosis was present. Foci of chronic inflammatory cells, including lymphocytes and plasma cells, were also evident. As a typical feature, we noted individual prominent hyalinized collagen bundles surrounded by tumour cells, predominantly in the periphery of the lesion (Fig. 1D). The mitotic count was 3 per 10 high-power fields (HPF).

Immunohistochemical staining revealed diffuse positivity for vimentin, factor XIIIa, CD68, CD163 (Fig. 1E) and CD44 (Fig. 1F). The lesion showed no reactivity for desmin, CD34, AE1/AE3, desmin, S-100 protein, α 1-antitrypsin or α 1-antichymotrypsin. Ki-67 staining showed less than 5% positive reactivity. Based on these findings, a diagnosis of atypical fibrous histiocytoma was made. As it was suspected that the initial resection may have left some residual tumour cells at depth, expanded excision with a 3-cm margin was performed one month later. At 30 months of follow-up, the patient was asymptomatic with no evidence of tumour recurrence.

Fig. 1. (A) Macroscopic view of the blackish-purple skin tumour on the right arm. (B) Dermal-subcutaneous tumour with focal extension into the subcutaneous tissue. The epidermis was hyperplastic and a grenz zone was evident (haematoxylin and eosin; HE \times 1). (C) The tumour is composed of a proliferation of interlacing fascicles of predominantly histiocyte-like eosinophilic spindle cells with vesicular nuclei. Abundant pleomorphic giant cells with huge bizarre nuclei are present (HE \times 100). (D) At the border of the lesion, the cells are interspersed with hyaline collagen bundles (HE \times 40). Immunohistochemical studies of the tumour cells. The cells were positive for (E) CD163 and (F) CD44.

© 2013 The Authors. doi: 10.2340/00015555-1563
Journal Compilation © 2013 Acta Dermato-Venereologica. ISSN 0001-5555

Acta Derm Venereol 93

738 Short communication

DISCUSSION

The distinctive histological features of AFH include a dermal lesion extending into superficial subcutaneous adipose tissue, composed of a population of pleomorphic spindled (fibroblast-like) and polyhedral (histiocyte-like) cells admixed with multinucleated giant cells, and macrophages as well as hemosiderin deposits. Kaddu et al. (2) reported the presence of 1–15 pathologic mitoses per 10 high power field (HPF) (mean 3.4 per 10 HPF) (20/59 cases, 33.9%) and/or geographic-like necrosis (7/59 cases, 11.9%) (2). Many reports have indicated positivity for factor XIIIa (4–6), but negativity has also been reported in some cases (2, 7, 8). Garrido-Ruiz et al. (6) and Wilk et al. (8) reported that AFH was CD34-negative. Although AFH of the skin is considered to be benign, there have been rare cases of multiple recurrence involving metastasis to the lymph nodes and lungs (2, 3, 5). Kaddu et al. (2) reported local recurrence in 3 of 21 cases for which follow-up was possible, and among these cases, distant metastasis occurred in 2. These 3 cases were all incompletely excised. Therefore, complete excision of AFH with a sufficient margin is important.

Histologically, the differential diagnosis of AFH includes DFSP, AFX and PDS/MFH. DFSP commonly occurs on the body trunk or proximal limbs of healthy adults, showing uniform bland spindle cells with spindle-shaped nuclei exhibit a storiform pattern and proliferate from the dermis to the subcutaneous adipose tissue with an unclear boundary, CD34 is diffusely positive, and immunoreactivity for α -SMA and desmin are usually negative (3, 9). In our case, as the tumour cells were notably polymorphic, CD34 was negative, and typical features of DF were observed in the background. AFX commonly occurs in sun-damaged skin of the head and neck in elderly individuals. AFX is similar to AFH in showing proliferation of spindle cells as well as multinucleated giant cells and bizarre cells (2). However, solar elastosis is observed in AFX, and a grenz zone is not evident because the tumour cells proliferate from directly under the skin. Moreover, features of typical DF are not observed (3). PDS/MFH commonly occurs in the limbs of middle-aged individuals, and it is common for the lesion to extend deeply into subcutaneous tissue, thus commonly forming a large tumour. An important point is that the tumour cells with profound atypia proliferate, and immunohistochemically do not demonstrate a specific line of differentiation. α 1-antitrypsin and α 1-antichymotrypsin are immunohistochemically positive in PDS/MFH (10). In the present case, the tumour cells were negative for both α 1-antitrypsin and α 1-antichymotrypsin, and atypia of the proliferating cells was not as severe as that in PDS/MFH.

Recent studies have shown that CD163 and CD44 are specific for DF and its variants. CD163, a haemoglobin scavenger receptor expressed by monocytes and tissue macrophages, is reportedly expressed in DF (89%) and cellular fibrous histiocytoma (100%), whereas it is negative in DFSP (83%) (11) and AFX (100%) (12). In addition, CD44 is the cell surface receptor for hyaluronate, and has also been reported to be a useful diagnostic marker of DF (13). In our case, the tumour cells showed strong expression of both CD163 and CD44, thus supporting the contention that AFH is a variant of DF.

ACKNOWLEDGEMENTS

The authors thank Professor Hiroshi Hashimoto, Department of Pathology, University of Occupational and Environmental Health, Japan, for his helpful comments on this case.

REFERENCES

- Fukamizu H, Oku T, Inoue K, Matsumoto K, Okayama H, Tagami H. Atypical ("pseudosarcomatous") cutaneous histiocytoma. *J Cutan Pathol* 1983; 10: 327–333.
- Kaddu S, Mc Menamin ME, Fletcher CD. Atypical fibrous histiocytoma of the skin. *Clinicopathologic analysis of 59 cases with evidence of infrequent metastasis*. *Am J Surg Pathol* 2002; 26: 35–46.
- Lever's histopathology of the skin. In: Elder DS, Elemtas R, Johnson BL, Murphy GF, Xu X, editors. Philadelphia: Lippincott Williams & Wilkins; 2009: p. 981.
- Huan Y, Vapnek J, Unger PD. Atypical fibrous histiocytoma of the scrotum. *Ann Diagn Pathol* 2003; 7: 370–373.
- Guilou L, Gebhard S, Salmeron M, Coindre JM. Metastasizing fibrous histiocytoma of the skin: a clinicopathologic and immunohistochemical analysis of three cases. *Mod Pathol* 2000; 13: 654–660.
- Garrido-Ruiz MC, Ramos P, Enguita AB, Rodriguez Peraltó JL. Subcutaneous atypical fibrous histiocytoma. *Am J Dermatopathol* 2009; 31: 499–501.
- Kuroda K, Tajima S. Proliferation of HSP47-positive skin fibroblasts in dermatofibroma. *J Cutan Pathol* 2008; 35: 21–26.
- Wilk M, Zelger BG, Nilles M, Zelger B. The value of immunohistochemistry in atypical fibrous histiocytoma. *Am J Dermatopathol* 2004; 26: 367–371.
- Aiba S, Tabata N, Ishii H, Ootani H, Tagami H. Dermatofibrosarcoma protuberans is a unique fibrohistiocytic tumor expressing CD34. *Br J Dermatol* 1992; 127: 79–84.
- Enzinger & Weiss's soft tissue tumors. In: Weiss SW, Goldblum JR, editors. Philadelphia: Mosby; 2008: p. 989.
- Sachdev R, Sundram U. Expression of CD163 in dermatofibroma, cellular fibrous histiocytoma, and dermatofibrosarcoma protuberans: comparison with CD68, CD34, and factor XIIIa. *J Cutan Pathol* 2006; 33: 353–360.
- Sachdev R, Robbins J, Kohler S, Vanchinathan V, Schwartz EJ, Sundram UN. CD163 expression is present in cutaneous histiocytomas but not in atypical fibroxanthomas. *Am J Clin Pathol* 2010; 135: 915–921.
- Calikoglu E, Augsburg E, Chavez P, Saurat JH, Kaya G. CD44 and hyaluronate in the differential diagnosis of dermatofibroma and dermatofibrosarcoma protuberans. *J Cutan Pathol* 2003; 30: 185–189.

Teleconsultation for the management of diabetes mellitus between Iwate Medical University and Miyako Prefectural Hospital

Yoshiniko Takahashi Jo Satoh

Division of diabetes and metabolism, Department of Internal Medicine, Iwate Medical University

要旨

岩手県において糖尿病患者数は毎年増加し、糖尿病が深刻化される人は平成25年度690万人と推計されたものが、平成26年度には200万人となり、さらに糖尿病の増え続ける患者をケアする必要があると認識されていると推測されている。糖尿病は慢性経過を辿る代謝性疾患であり、慢性経過を辿ることで合併症・併発症の多くなるため、大規模な遠隔医療・遠隔診療が糖尿病の診療に必要であると考えられている。本研究は、糖尿病の診療に必要であると考えられている遠隔医療・遠隔診療の導入を目的として、岩手医科大学と県立宮古病院の間で糖尿病の遠隔診療支援システムを構築した。今後長期的な見込みの患者を対象に参加者を募り、診療支援を開始したいと考えている。

Keywords: teleconsultation, diabetes mellitus, virtual private network

1. はじめに

日本における糖尿病患者数は毎年増加し、糖尿病が深刻化される人は平成25年度690万人と推計されたものが、平成26年度には200万人となり、さらに糖尿病の増え続ける患者をケアする必要があると認識されていると推測されている。糖尿病は慢性経過を辿る代謝性疾患であり、慢性経過を辿ることで合併症・併発症の多くなるため、大規模な遠隔医療・遠隔診療が糖尿病の診療に必要であると考えられている。本研究は、糖尿病の診療に必要であると考えられている遠隔医療・遠隔診療の導入を目的として、岩手医科大学と県立宮古病院の間で糖尿病の遠隔診療支援システムを構築した。今後長期的な見込みの患者を対象に参加者を募り、診療支援を開始したいと考えている。

いることと、通常の診療診療を促進するためには医師の直接診療が必要となるがであった。このために、遠隔診療にも診療報酬が適用されるようにするため、遠隔診療に必要となる医師、施設における設備、患者との関係性などを検討し、必要な設備を整えることとした。岩手医科大学と県立宮古病院の間で糖尿病の遠隔診療支援システムを構築し、今後の診療支援を開始したいと考えている。

2. 方法

プロジェクトの具体的な内容としては、岩手医科大学病院と岩手医科大学附属病院、代謝内科と糖尿病・代謝内科、岩手医科大学と県立宮古病院の間で糖尿病の遠隔診療支援システムを構築し、今後の診療支援を開始したいと考えている。

現在までのところ、必要設備の整備およびシステムを完了したものの、患者のサポートを調整したばかりであり、今後の診療支援に必要となる設備の整備、遠隔診療に関するレギュレーションの整備などが必要である。

3. 結果と考察

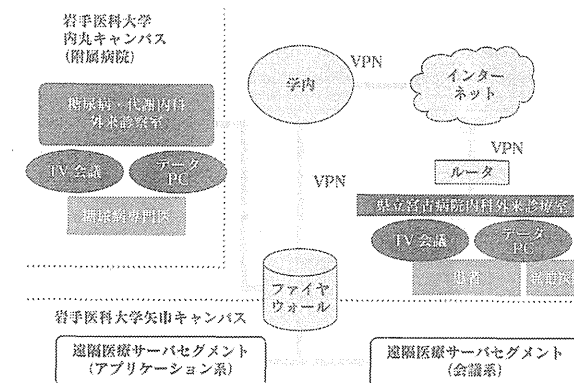


図1 構築された糖尿病遠隔診療システム

カメラを用いたリアルタイムの手法の方が、医師従事者の負担が小さく、コストなどの面で優れているという。遠隔診療状況については、teleconsultationを遠隔診療よりも広いという認識は必要だが、特に慢性経過を辿る糖尿病患者の割合が高くなるため、遠隔診療の導入は必要である。

参考文献

1) Verheoven F, Tanja Dijkstra K, Nijland M, et al. Asynchronous and Synchronous Teleconsultation for Diabetes Care: A Systematic Literature Review. J Diabetes Sci Technol 2010; 4(3): 666-684.

江原 茂

岩手医科大学医学部放射線医学講座

Prefecture-level wide area network to support imaging diagnosis in the area hit by the earthquake and tsunami

Shigeru Ehara

Department of Radiology, Iwate Medical University, School of Medicine

要約

震災による被災医療機関の支援として画像診断の遠隔診断に加えて、広域ネットワークによる被災医療施設との画像情報連携・画像診断支援の推進に努め、最終的には内陸の中核病院を含めた県全域での画像情報ネットワークの構築を目指す。このような試みは国内での先行例がないが、前掲課題などに照らした際の留意点を用いたから実践に進展の必要がある。

キーワード：遠隔画像診断、広域ネットワーク、画像情報連携

1. 背景

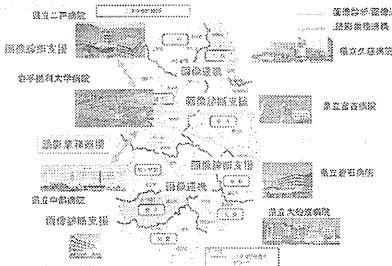
大規模震災で CT といった放射線機器は電源供給に大きく依存しており、震災時には容易に機能しない。さらに震災による被災医療機関の稼働停止や電源供給の途絶による大きな被害が存在する。5月11日その時点で、被災地では放射線装置では電源供給が断たれることにより稼働する放射線装置には震災の危険が生じる。被災への課題だけでなく、超広域ネットワークによる被災医療機関間の連携も重要な課題となっている。

その一方、1990年代以降普及されてきた PACS の形式による画像データ・フォーマットの共通化や非圧縮による画像診断システムの稼働への向きは、異なる機器や装置で得られた画像情報が互換の基盤で保存・運用することを可

能にし、広域ネットワークによる超域レベルでの画像情報の共有化や管理を可能にしている。クラウドを利用した画像管理サービスへの移行も震災による被災の危険の少ない画像情報共有が可能になっている。さらには学会などで遠隔画像診断の発展を目指す議論が行われており、環境整備はすでに進んでいる上、

2. 画像情報ネットワークの現状

岩手県の面積が大きく内陸の医療機関が広く分散していることから、岩手医科大学医学部放射線医学講座では被災医療機関の県内機関への対応に限っては、遠隔診断への移行を少しずつ進めてきた。平成25年3月の再発では、相互連携病院、県立中央病院の臨床を岩手医科大学附属病院中央診療部に置き実施を行っているが、画像情報の共



【図1】ネットワークの図解と付録

Japanese Journal of Information and Telemedicine Vol. 9 (1)

共有化まで進んでいない。画像情報は従来の CD や DVD による搬送に依存している。被災地医療機関については、画像情報の物理的な搬送による課題を克服してきている。

3. 広域ネットワークによる画像診断支援体制の構築に向けて

被災医療機関の目的は被災医療機関における画像診断支援体制の構築にあるが、具体的には以下の2点になる。すなわち、

- 1) 被災地被災医療機関 (通常 4 中核病院) との画像情報ネットワーク構築による画像診断の共有化と診断支援
- 2) 地域連携の推進による内陸の岩手県立の中核病院も含めた県全体の画像情報支援体制の構築と強化

これらの実現は平成25年度から具体的な事業に入ることを前提とする。その第一の目標は、被災中核病院との画像情報共有化を図るネットワークの構築と、被災地医療機関を含む被災地医療機関間の画像情報共有化を図ることである。画像情報共有化の推進を促したその研究共有その一である【図1】。

画像情報広域ネットワークの構築はアメリカでは多くの例があるが、国内では単独では存在していない。岩手県の県立4病院との画像情報連携の推進と前掲の共有化はそれぞれのモジュールになることが期待される。画像診断支援の機材と担当を岩手・盛石の2病院との間で分け、それぞれの内陸施設との画像情報共有化の推進を県庁のシステムに組み込むことにより、画像情報および画像診断支援の共有化を進めていく方針である。被災地への支援の枠組みを構築して可能な限りコンサルテーションの範囲を拡大していくこと。また内陸の中核病院への支援を促して内陸の画像情報の共有化をさらに進めることにより、被災地の画像情報の共有化と画像診断支援体制を構築することの臨床目標である。

4. 画像データ管理体制の問題点

現在考えられる画像データ管理体制としては、必要最小限のデータの確保は各病院で行うこと、保存期間の短縮データを岩手医科大学センターにおくこと、主要施設に利用するための画像データ (レポートを含む) の共有化を確保に努めることを考えている。異なる医療機関にまたがる患者の同一性の確保はデータセンターで十分に留意して確保に努める必要がある。アメリカの社会保険制度のような共通番号のない状況において、異なるシステムでの同一患者の同一性については、氏名と生年月日だけで取り扱えるが、厳格的には医師の判断が必要である。一つの課題としては、臨床に手動で入力されたデータには患者本人の可能性が比較的高いことがあり、また診療報酬ごとにデータ管理のレベルが異なるため、データの共有化に際しては必要なものから慎重に選別する必要がある。このようなデータ管理の実際的な運用については経験が不十分な点が多く、これらの経験が行われる。

5. 最後に

広域ネットワークによる被災医療機関との画像情報連携・画像診断支援の推進により、最終的には内陸の中核病院を含めた県全域での画像情報ネットワークの構築を目指す。このような試みは、国内での先行例がないが、前掲課題

を抽出しながら実践に努める必要がある。

参考文献

- 1) 江原茂 遠隔画像診断システム導入の目的と画像診断のありかた、臨床放射線 2012; 57: 1144-1144.

Japanese Journal of Information and Telemedicine Vol. 9 (1)

2. Dibbern DA Jr, Loevner LA, Lieberman AP, Salhani KE, Freese A, Marcotte PJ. MR of thoracic cord compression caused by epidural extramedullary hematopoiesis in myelodysplastic syndrome. *Am J Neuroradiol*. 1997; 18: 363–366.
3. Mateen FJ, Harding SR, Saxena A. Extensive myocardial infiltration by hemopoietic precursors in a patient with myelodysplastic syndrome. *BMC Blood Disord*. 2006; 6: 4.

Small-cell carcinoma of the breast with squamous differentiation

DOI: 10.1111/phis.12201

© 2013 John Wiley & Sons Ltd

Sir: The WHO classifies mammary carcinomas with neuroendocrine (NE) features as a special tumour entity representing <1% of invasive breast carcinomas.¹ Small-cell carcinoma of the breast is a rare NE subtype that may show aggressive clinical behaviour, whereas the other, more frequent, breast carcinomas with NE differentiation (cellular mucinous carcinoma and solid papillary carcinoma) are usually of low grade. To our knowledge, there is only one brief description concerning metaplastic change in these NE cancers.² Herein, we report an exceptionally rare small-cell mammary carcinoma showing squamous differentiation.

The patient, a 58-year-old postmenopausal Japanese woman, presented with a palpable mass in the upper outer quadrant of the right breast. Her family history included a sister with ovarian cancer. Ultrasonography revealed a well-defined, focally distorted, hypo-echoic right breast tumour. Systemic CT detected no other suspicious lesions. We performed ultrasound-guided, fine needle aspiration of the breast lesion, and the cytological diagnosis was carcinoma.

The cut surface of the mastectomy specimen contained a lobulated grey-whitish tumour, measuring 45 × 40 × 40 mm. Histopathologically, this invasive tumour was composed of solid and/or trabecular growths of densely packed, small to medium-sized carcinoma cells with well-developed vascular stroma (Figure 1A,B). Focal coagulation necrosis and haemorrhage were present. Carcinoma cells were polygonal or occasionally spindle-shaped, with high nuclear/cytoplasmic ratios and ovoid nuclei with finely granular chromatin and absent or inconspicuous nucleoli (Figure 1B). Mitotic figures were numerous [82 per 10 high-power fields (HPFs)]. Squamous differentiation, i.e. formation of nests of polygonal carcinoma cells with abundant, eosinophilic cytoplasm and intercellular bridging with focal keratin pearls, was found (Figure 1C). Mitotic activity was

also present in this squamous component, but was lower (12 per 10 HPFs) than that in the small-cell component. Focal lymphatic permeation was detected. An *in-situ* ductal carcinoma component, predominantly showing cribriform architecture, and with comedo necrosis, was observed within and near the tumour mass (Figure 1A,D). No metastases were identified in the 18 excised right axillary lymph nodes.

Immunohistochemically, invasive carcinoma cells were diffusely positive for synaptophysin and CD56 (neural cell adhesion molecule, NCAM) and focally positive for chromogranin A, whereas cells showing squamous metaplasia were negative or weakly positive and *in-situ* cells were negative for these NE markers (Figure 2A). Carcinoma cells were diffusely positive for cytokeratin 7 and negative for cytokeratin 20. High molecular weight cytokeratin (34βE12) was clearly demonstrated only in carcinoma cells with squamous metaplasia (Figure 2B). Gross cystic disease fluid protein 15 (GCDFFP15) was identified in 2% of the invasive carcinoma cells and in 20% of the *in-situ* carcinoma cells (Figure 2C). The tumour was oestrogen receptor-negative in both invasive and *in-situ* areas, whereas weak progesterone receptor reactivity was detected in the invasive carcinoma nuclei (positive cell rate: 1.5%), and the *in-situ* component was progesterone receptor negative. The HER2 score was estimated at 1+, and the MIB-1 labelling index was 51.4%.

Reverse-transcriptase polymerase chain reaction (RT-PCR) analysis revealed overexpression of chromogranin A mRNA in the invasive cancer tissue.

Postoperatively, the patient received doxorubicin (60 mg/m²) and cyclophosphamide (600 mg/m²) every 4 weeks for four cycles as adjuvant chemotherapy. She remains alive and well, with neither recurrence nor metastasis, 49 months after surgery.

The possibility of metastatic small-cell carcinoma from another site should be ruled out.¹ Imaging and clinical history confirmed that our patient had no lesions in other organs, and an *in-situ* component accompanying the invasive breast cancer was demonstrated histologically. These are regarded as the two most important features for diagnosing primary small-cell mammary carcinoma.^{2,3} In addition, GCDFFP15 immunoreactivity supports a diagnosis of primary NE carcinoma of the breast, despite oestrogen receptor negativity.⁴ Furthermore, mammary NE carcinomas are generally cytokeratin 7-positive and cytokeratin 20-negative, whereas pulmonary small-cell carcinoma is negative for both.^{1,2}

It has been suggested that mammary NE carcinomas generally result from a divergent differentiation

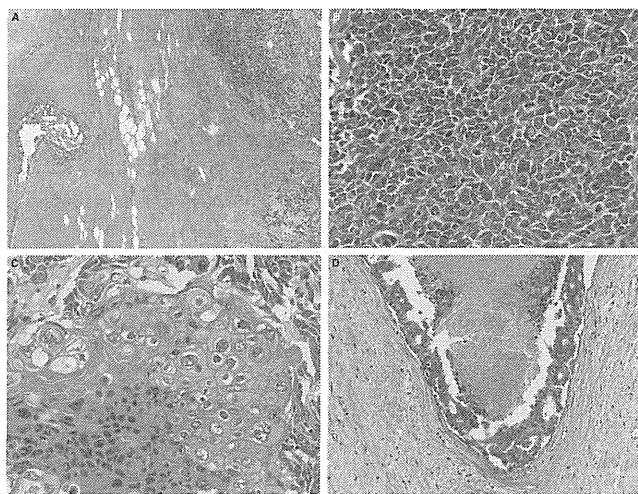


Figure 1. Histological findings of small-cell mammary carcinoma with squamous differentiation. A, Invasive region (right side) and proximally located *in-situ* component (left side). B, Cancer cells showing medullary invasive growth with a capillary network are polygonal or mildly fusiform in shape, and have relatively scant cytoplasm and hyperchromatic nuclei with frequent mitoses. C, Note the nest composed of polygonal cancer cells with abundant, eosinophilic and/or clear cytoplasm, irregularly shaped nuclei, and keratinization. D, *In-situ* component composed of ductal cancer cells arranged in glandular structures, with central necrosis.

event in breast cancer, because normal NE cells are almost never found in the breast,^{5,6} whereas we recently described a hyperplastic condition of NE cells that was possibly relevant to the development of some mammary NE carcinomas.⁶ In the present case, the *in-situ* ductal carcinoma component had no NE features, immunohistochemically or morphologically, and no normal-like and/or hyperplastic NE cells were detected in background breast tissue. It is thus reasonable to speculate that the breast cancer in this case acquired a small-cell NE nature divergently when *in-situ* cancer cells invaded surrounding stromal tissue or thereafter.

Papotti *et al.* reported that three of four patients with primary small-cell carcinoma of the breast died within 15 months after initial diagnosis, and,

accordingly, that this type of tumour could represent an aggressive variant of breast cancer,³ whereas Shin *et al.* emphasized that an important determinant of the outcome is the disease stage at the time of diagnosis.² In addition, invasive breast carcinomas with metaplastic features generally have a poor prognosis.⁷ Interestingly, our patient with a highly unusual mammary small-cell carcinoma showing squamous metaplasia has remained alive and well for more than 4 years to date, with the standard treatment for operable infiltrating breast cancers. Despite the local tumour being large and the presence of vascular invasion, there was no evidence of lymph node or distant spread of the cancer (stage IIA), which may account for the patient's survival in this case.

Histopathology, 63, 738–741.

ACKNOWLEDGEMENTS

Tomonori Kawasaki is on sabbatical leave from the University of Yamanashi, and is supported by Yamanashi University Characteristic Prior Research Funds and Grants-in-Aid for Scientific Research (No. 23790394 and No. 25460414) from the Japanese Ministry of Education, Culture, Sports, Science and Technology. This work is also supported by Persother Project (Contract SMIS-CSNR; 549/12.024) funds granted to Gianni Bussolati.

Tomonori Kawasaki^{1,2}
Gianni Bussolati^{1,3}
Isabella Castellano¹
Caterina Marchio¹
Lorenzo Daniele¹
Luca Molinaro¹
Tetsuo Kondo²
Ryohei Katoh²
Shingo Inoue²
Hideki Fujii⁴
Tamotsu Sugai⁵
Anna Sapino¹

¹Department of Medical Sciences, University of Turin, Turin, Italy, ²Department of Pathology, University of Yamanashi, Yamanashi, Japan, ³Institute 'Victor Babes', Bucharest, Romania, ⁴First Department of Surgery, University of Yamanashi, Yamanashi, and ⁵Department of Molecular Diagnostic Pathology, Iwate Medical University School of Medicine, Morioka, Japan

- Bussolati G, Badve S. Carcinomas with neuroendocrine features. In Lakhani SR, Ellis IO, Schnitt SJ, Tan PH, van de Vijver MJ eds. *World Health Organization classification of tumours of the breast*. Lyon: IARC Press, 2012: 62–63.
- Shin SJ, DeLellis RA, Ying L, Rosen PP. Small cell carcinoma of the breast: a clinicopathologic and immunohistochemical study of nine patients. *Am J Surg Pathol*. 2000; 24: 1231–1238.
- Papotti M, Gherardi G, Eusebi V, Pagani A, Bussolati G. Primary oat cell (neuroendocrine) carcinoma of the breast. Report of four cases. *Vitrolos J Arch Pathol Anat Histopathol*. 1993; 42B: 103–108.
- Sapino A, Right L, Cassoni P, Papotti M, Gugliotta P, Bussolati G. Expression of apocrine differentiation markers in neuroendocrine breast carcinomas of aged women. *Mod Pathol*. 2001; 14: 768–776.
- Bussolati G, Gugliotta P, Sapino A, Eusebi V, Lloyd RV. Chromogranin-reactive endocrine cells in argyrophilic carcinomas ('carcinoids') and normal tissue of the breast. *Am J Pathol*. 1985; 120: 186–192.
- Kawasaki T, Mochizuki K, Yamauchi H *et al.* Neuroendocrine cells associated with neuroendocrine carcinoma of the breast: nature and significance. *J Clin Pathol*. 2012; 65: 699–703.

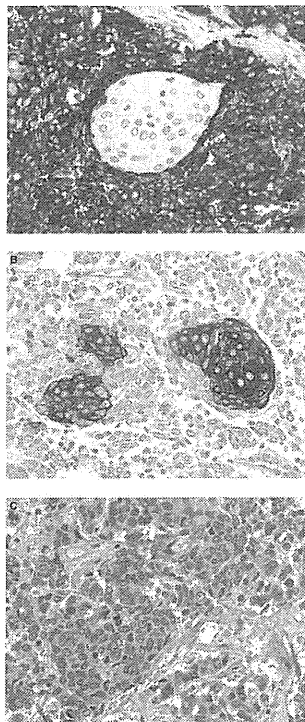


Figure 2. Immunohistochemical findings of small-cell mammary carcinoma with squamous differentiation. A, Synaptophysin immunohistochemistry is diffusely positive in most invasive cancer cells, but the component showing squamous differentiation is negative. B, In contrast, 34βE12 stains only areas showing squamous differentiation. C, Scattered GCDFFP15-expressing cancer cells are observed in the invasive lesion.

菅井 有¹ 湯井 高志²

岩手医科大学医学部病理学講座分子診断病理学分野¹ 岩手医科大学理学部先進医療病理学分野²

Telepathology in an earthquake disaster
— A proposal for Iwate Model —

Yu Suga¹ Takashi Sawai²

Department of Molecular Diagnostic Pathology, Iwate Medical University

要約

東北地方は平成 23 年 3 月 11 日に東日本大震災により大規模な被害を受けた。それによって被災地の医療は大幅的な打撃を受けた。今後の医療支援が重要となる。今回のような津波と地震による被災地は、前記不備を補償する必要がある。これまでの遠隔病理診断システムは、被災地の医療支援に有効でなかった。今回の災害発生から改めて遠隔病理診断システムに必要と認識する。今後は遠隔病理診断システムの構築が重要となる。

キーワード: テレパソロジー、遠隔病理診断、病理情報システム、震災

1. はじめに

平成 23 年 3 月 11 日に東北地方太平洋沖地震が発生した。宮城県を中心に津波と地震による甚大な被害を受けた。多くの人命が奪われた。この際、被災地の医療機関も同様の被害を受けた。その被害は被災地だけでなく、被災地の医療機関から被災地まで影響を及ぼすと考えられる。今回のような被災地は、前記不備を補償する必要がある。今回の災害発生から改めて遠隔病理診断システムに必要と認識する。今後は遠隔病理診断システムの構築が重要となる。

被災地は被災地であるが、被災地から被災地まで影響を及ぼす可能性がある。今回のような被災地は、前記不備を補償する必要がある。今回の災害発生から改めて遠隔病理診断システムに必要と認識する。今後は遠隔病理診断システムの構築が重要となる。

3. 地震による被害

地震による被害は、被災地だけでなく、被災地から被災地まで影響を及ぼす可能性がある。今回のような被災地は、前記不備を補償する必要がある。今回の災害発生から改めて遠隔病理診断システムに必要と認識する。今後は遠隔病理診断システムの構築が重要となる。

4. 震災に強い病理診断システムの構築

上記の理由から、今回のような津波と地震による被災地から、被災地から被災地まで影響を及ぼす可能性がある。今回のような被災地は、前記不備を補償する必要がある。今回の災害発生から改めて遠隔病理診断システムに必要と認識する。今後は遠隔病理診断システムの構築が重要となる。

2. 津波による被害の特徴

津波の被害は、被災地だけでなく、被災地から被災地まで影響を及ぼす可能性がある。今回のような被災地は、前記不備を補償する必要がある。今回の災害発生から改めて遠隔病理診断システムに必要と認識する。今後は遠隔病理診断システムの構築が重要となる。

10. Japanese Journal of Telemedicine and Telecare Vol. 9 (2)

ガラス板を電子化することが可能になる。そうすれば、被災地は被災地であるが、被災地から被災地まで影響を及ぼす可能性がある。今回のような被災地は、前記不備を補償する必要がある。今回の災害発生から改めて遠隔病理診断システムに必要と認識する。今後は遠隔病理診断システムの構築が重要となる。

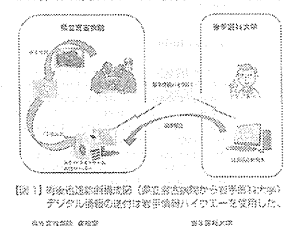
電子化されたガラス板を電子化することが可能になる。そうすれば、被災地は被災地であるが、被災地から被災地まで影響を及ぼす可能性がある。今回のような被災地は、前記不備を補償する必要がある。今回の災害発生から改めて遠隔病理診断システムに必要と認識する。今後は遠隔病理診断システムの構築が重要となる。

ガラス板の電子化は、被災地だけでなく、被災地から被災地まで影響を及ぼす可能性がある。今回のような被災地は、前記不備を補償する必要がある。今回の災害発生から改めて遠隔病理診断システムに必要と認識する。今後は遠隔病理診断システムの構築が重要となる。

被災地は被災地であるが、被災地から被災地まで影響を及ぼす可能性がある。今回のような被災地は、前記不備を補償する必要がある。今回の災害発生から改めて遠隔病理診断システムに必要と認識する。今後は遠隔病理診断システムの構築が重要となる。

被災地は被災地であるが、被災地から被災地まで影響を及ぼす可能性がある。今回のような被災地は、前記不備を補償する必要がある。今回の災害発生から改めて遠隔病理診断システムに必要と認識する。今後は遠隔病理診断システムの構築が重要となる。

被災地は被災地であるが、被災地から被災地まで影響を及ぼす可能性がある。今回のような被災地は、前記不備を補償する必要がある。今回の災害発生から改めて遠隔病理診断システムに必要と認識する。今後は遠隔病理診断システムの構築が重要となる。



【図 1】 被災地と被災地を結ぶ遠隔病理診断システム構築の概要図

【図 2】 被災地と被災地を結ぶ遠隔病理診断システム構築の概要図

【図 3】 被災地と被災地を結ぶ遠隔病理診断システム構築の概要図

参考文献

1) Sawaf Y, Utsui M, Kamaishi A, et al. The state of telepathology in Japan. J Pathol Inform. 2010 Aug 10; 1.
2) Bellis M, Mathis S, Nuglar C, et al. Digital pathology: Activities and practices in the Canadian pathology community. J Pathol Inform. 2012 Mar 14; 4: 3.
3) Liu JT, Loewke NG, Mandella M, et al. Real-time pathology through in vivo microscopy. Stud Health Technol Inform. 2013; 185: 235-44.
4) Bueno C, Garcia-Rojas M, D'Amico O, et al. Emerging uses: grid technology in pathology. Stud Health Technol Inform. 2012; 179: 213-29.
5) Heuser A. Digital pathology for education. Stud Health Technol Inform. 2011; 179: 68-71.

Japanese Journal of Telemedicine and Telecare Vol. 9 (2) 11

Case Report

Electrical storm after cardiac resynchronization therapy in a patient with nonischemic cardiomyopathy: Signal-averaged vector-projected 187-channel electrocardiogram-based risk stratification for lethal arrhythmia

Toshiko Nakai, MD^{a,*}, Hiroaki Mano, MD^b, Yukitoshi Ikeya, MD^a, Kazumasa Sonoda, MD^a, Sonoko Ashino, MD^a, Yasuo Okumura, MD^a, Kimie Ohkubo, MD^a, Satoshi Kunimoto, MD^a, Yuji Kasamaki, MD^a, Ichiro Watanabe, MD^a, Atsushi Hirayama, MD^a, Kenji Nakai, MD^b

^a Division of Cardiology, Department of Medicine, Nihon University School of Medicine, 30-1 Oyaguchi-kami-cho, Inbashi-ku, Tokyo 173-8610, Japan

^b Department of Internal Medicine of Dentistry, Iwate Medical University, Japan

ARTICLE INFO

Article history:
Received 23 April 2013
Received in revised form
2 May 2013
Accepted 9 May 2013
Available online 5 July 2013

Keywords:

CRT
Proarrhythmia
RTc dispersion
Tpeak-end dispersion

ABSTRACT

We describe treatment of atrial flutter and electrical storm presenting as incessant ventricular tachycardia (VT) after implantation of a cardiac resynchronization therapy defibrillator (CRT-D) in a patient with dilated cardiomyopathy. No prior arrhythmic event had occurred. Our treatment strategy, including amiodarone administration, was guided in part by signal-averaged vector-projected 187-channel electrocardiogram (SAVP-ECC)-based risk stratification for ventricular arrhythmia. Corrected recovery time (RTc) dispersion and Tpeak-end dispersion were used to evaluate transmural dispersion of repolarization. RTc and Tpeak-end dispersion increased during the period of electrical storm. Values were improved 2 years after CRT-D implantation, and the amiodarone was discontinued. The VT has not recurred despite discontinuation of the antiarrhythmic agent. SAVP-ECC-based risk stratification for ventricular arrhythmia proved useful for the management of antiarrhythmic therapy.

© 2013 Japanese Heart Rhythm Society. Published by Elsevier B.V. All rights reserved.

1. Case report

A 77-year-old man with dilated cardiomyopathy visited our hospital in December 2010 and reported dyspnea on effort. Echocardiography revealed cardiac dyssynchrony with a low ejection fraction of 20%, and the patient was diagnosed with New York Heart Association class III heart failure. The plasma N-terminal pro-B-type natriuretic peptide (NT-pro BNP) level was 3691 pg/mL. The electrocardiogram (ECG) QRS complex (136 ms) was widened to 136 ms, with a left bundle branch block contour (Fig. 1). The patient was being treated with spironolactone (aldactone), β -blocker (carvedilol), and angiotensin II receptor antagonist (captopril). Implantation of a cardiac resynchronization therapy defibrillator (CRT-D) was scheduled and performed in May 2011, without any complications. After implantation of the right ventricular (RV) lead in the RV apex, coronary venography was performed, and a suitable lateral branch was identified as a candidate vessel for left ventricular (LV) lead implantation. The LV lead was positioned at the midportion of the lateral branch. The LV pacing threshold was 0.5 V at 0.5 ms without phrenic nerve stimulation. The right atrial

(RA) lead was then positioned at the RA appendage. The following device and leads were used: Promote RF generator, Durata 7120Q RV defibrillation lead, QuickFlex 1158T LV lead, and Tendril STS RA lead (St. Jude Medical, St. Paul, Minnesota, USA). The RV pacing threshold was 0.75 V at 0.4 ms, and the RA pacing threshold was 0.5 V at 0.4 ms. The device was programmed with a ventricular tachycardia (VT) zone set to ≥ 166 bpm (therapies = antitachy pacing (ATP) $\times 3$, shock 10 J, 25 J, 36 J $\times 4$) and a ventricular fibrillation (VF) zone set to ≥ 230 bpm (therapies = shock 15 J, 36 J, 36 J $\times 4$).

After CRT-D implantation, the QRS duration decreased to 122 ms (Fig. 2), and the cardiac dyssynchrony improved. However, 5 days after implantation, atrial flutter (AFL) and electrical storm presenting as frequent VT were seen. As shown in Fig. 2A, the VT was initiated by a premature ventricular complex. The CRT-D intracardiac tracing showed both AFL and VT. Appropriate shocks were delivered, and both the AFL and VT were terminated (Fig. 3B); however, incessant VT developed after restoration of sinus rhythm. A total of 9 VT zone shocks were delivered. Biventricular pacing was discontinued, and intravenous administration of amiodarone was initiated to inhibit VT. The VT abated within 1 week, and CRT was restarted. Oral amiodarone was administered to prevent VT recurrence. To determine the risk of ventricular arrhythmia, we evaluated the corrected recovery time (RTc) dispersion and Tpeak-end dispersion on a signal-averaged vector-projected 187-channel electrocardiogram

* Corresponding author. Tel.: +81 33972 8111x2412; fax: +81 33972 1098.
E-mail address: nakai.toshiko@nihon-u.ac.jp (T. Nakai).

1880-4275/\$ - see front matter © 2013 Japanese Heart Rhythm Society. Published by Elsevier B.V. All rights reserved.
http://dx.doi.org/10.1016/j.joa.2013.05.004



Fig. 3. Cardiac monitor tracing and intracardiac electrocardiogram shows atrial fibrillation and ventricular tachycardia episodes 5 days after CRT-D implantation.

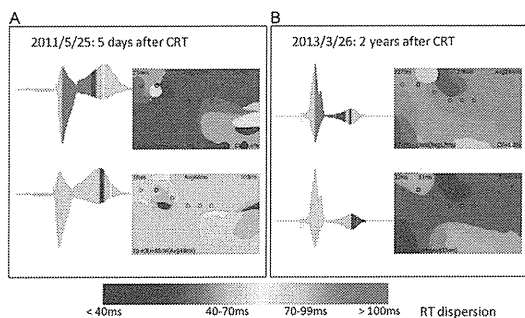


Fig. 4. RTc and Tpeak-end dispersion assessed on SAVP-ECC obtained 5 days and 1 year after CRT implantation. RTc and Tpeak-end dispersion were improved 2 years after CRT implantation.

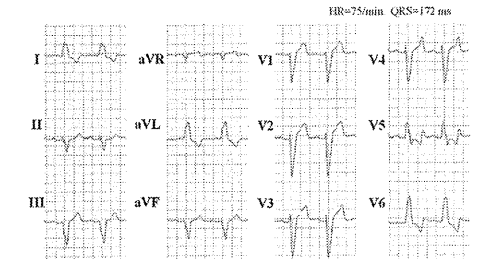


Fig. 1. Twelve-lead electrocardiogram obtained before CRT shows a wide QRS complex with left bundle branch block.

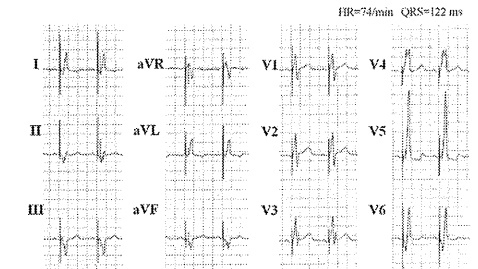


Fig. 2. Twelve-lead electrocardiogram obtained after CRT shows narrowing of the QRS complex compared to that before CRT.

(SAVP-ECC). RTc and Tpeak-end dispersion increased during the period of electrical storm (average, 15 ms and 48 ms, respectively; Fig. 4A). These findings suggest that transmural dispersion of repolarization increased in our patient, leading to ventricular proarrhythmia. Two years after implantation of CRT-D, follow-up SAVP-ECC showed decreased augmentation of RTc dispersion and Tpeak-end dispersion (17 ms and 13 ms, respectively; Fig. 4B). It remains unclear whether this improvement was the result of time or the administration of amiodarone. We halved the dose of amiodarone before withdrawing the drug altogether. No VT recurrence occurred despite discontinuation of the antiarrhythmic agent.

2. Discussion

Proarrhythmic events after CRT have been reported in 5–10% of CRT recipients [1–4]. Gasparini et al. investigated the incidence of electrical storm in patients with heart failure treated with CRT and reported an increased incidence in patients with nonischemic cardiomyopathy in whom a CRT-D was implanted for secondary prevention [5]. In most cases, the arrhythmia can be managed by

administration of an antiarrhythmic agent and/or discontinuation of LV pacing within 1 month after implantation of the CRT system. Kantharia et al. reported a case of electrical storm induced by CRT. The VT did not disappear even after extraction of the LV lead, and catheter ablation was performed to control the VT [6]. In another case, VT was induced by biventricular pacing and controlled by triple-site biventricular pacing and atrioventricular node ablation [7]. In contrast, CRT has been reported to suppress arrhythmias in some cases [8–10]. These reports suggest that the suppression is not due to the effects of pacing itself. Rather, reverse remodeling with CRT can decrease the AFL burden and frequency of ventricular arrhythmias.

The mechanism underlying the proarrhythmic effect of CRT is not well understood. One explanation is that transmural dispersion of repolarization increases with LV pacing. Bai et al. studied the effects of LV epicardial pacing and biventricular pacing in a canine model of dilated cardiomyopathy [11] and showed that both LV epicardial pacing and biventricular pacing prolonged the ventricular repolarization time and increased transmural dispersion of repolarization. Prolonged transmural dispersion occurred parallel to augmentation in the Tpeak-end interval. According to Scott et al., CRT with transseptal

endocardial LV pacing (in comparison with epicardial LV pacing) reduced QTc and Tpeak-end dispersion, and these authors concluded that transseptal LV pacing may be less arrhythmogenic [12]. Barhaiya et al. looked at the relationship between ventricular arrhythmia, the QT interval, and Tpeak-end dispersion and found that increases in Tpeak-end dispersion and Tpeak-end/QT ratio were associated with an increased incidence of ventricular arrhythmia in patients with a CRT-D [13]. Another group also reported an association between Tpeak-end dispersion and major arrhythmic events [14].

Nakai et al. showed that RTc and Tpeak-end dispersion can be used to evaluate the spatial distribution of myocardial repolarization [15,16]. We measured RTc and Tpeak-end dispersion in the acute and chronic periods in the case reported herein. Both variables were increased during the acute period after CRT, suggesting that repolarization heterogeneity was augmented before being modified by amiodarone. These changes are consistent with previous reports of prolongation of the Tpeak-end interval with LV pacing. On the follow-up SAVP-ECC, RTc and Tpeak-end dispersion had decreased to within safe ranges. There is no standard index for use of antiarrhythmic agents, and it is difficult to make the decision to stop an antiarrhythmic agent once it is started, even if the patient is free of arrhythmia. In the present case, RTc/Tpeak-end dispersion increased in the acute phase after CRT, suggesting a potential substrate for ventricular arrhythmia, but both measures decreased to within normal range with amiodarone administration and with time. We controlled the dose of amiodarone in response to the low risk for ventricular arrhythmia indicated by the SAVP-ECC. Our experience in this case highlights the importance of risk stratification for lethal arrhythmia after CRT.

3. Conclusion

We treated a patient who experienced electrical storm after CRT-D implantation. Our treatment strategy was guided in part by SAVP-ECC-based risk stratification for ventricular arrhythmia. Our SAVP-ECC findings indicate that the proarrhythmic effect of CRT may be due to repolarization heterogeneity induced by LV pacing. The SAVP-ECC findings allowed us to both administer and withdraw the antiarrhythmic agent effectively; therefore, we suggest use of SAVP-ECC as a risk stratification tool in cases of CRT-induced electrical storm.

Conflict of interest

There is no conflict of interest related to this report.

References

- Albert CM. Cardiac resynchronization therapy and proarrhythmia: weathering the storm. *Circulation* 2005;112:1713–9.
- Rozin F, Noda J, Aiba T, et al. Cardiac resynchronization therapy to prevent life-threatening arrhythmias in patients with congestive heart failure. *J Electrocardiol* 2011;42:385–91.
- Shenoi S, Choudhry GM, Grew M, et al. Potential nonarrhythmic effect of biventricular pacing: fact or myth? *Heart Rhythm* 2005;2:2051–8.
- Ilkhanian M, Khanlou M, Arashi H, et al. Effects of cardiac resynchronization therapy on the arrhythmic substrate in a patient with long QT and unexplained syncope. *J Arrhythmia* 2011;27:222–7.
- Gasparini M, Lunati M, Landolina M, et al. Electrical storm in patients with biventricular implantable cardioverter defibrillator incidence, predictors, and prognostic implications. *Am Heart J* 2009;158:247–54.
- Kantharia DK, Patel JA, Nigam BS, et al. Electrical storm of monomorphic ventricular tachycardia after a cardiac resynchronization therapy-defibrillator upgrade. *Europace* 2010;12:633–6.
- Hiroki S, Yoshida A, Itoji A, et al. Electrical storm after cardiac resynchronization therapy suppressed by triple-site biventricular pacing and atrioventricular node ablation. *Heart Rhythm* 2012;9:2038–42.
- Wakino S, Itoyama T, Itoji A, et al. Usefulness of suppression of ventricular arrhythmias by biventricular pacing in severe congestive cardiac failure. *Am J Cardiol* 2006;98:231–2.
- Lavoie C, Heit JG, Santini M. Atrial tachyarrhythmias and cardiac resynchronization therapy: clinical and therapeutic implications. *Heart* 2010;96:1474–8.
- Shimizu S, Shigemitsu H, Takano S. The effect of left ventricular (LV) remodeling on ventricular arrhythmia in cardiac resynchronization therapy (CRT)-eligible patients: antiarrhythmic effect of CRT. *Pacing Clin Electrophysiol* 2012;35:282–7.
- Bai R, Lu J, Fu J, et al. Left ventricular epicardial activation increases transmural dispersion of repolarization in healthy, long QTc and dilated cardiomyopathy dogs. *Pacing Clin Electrophysiol* 2005;28:1983–90.
- Scott AD, Van AM, Vinters E, et al. Transseptal left ventricular endocardial pacing reduces dispersion of ventricular repolarization. *Pacing Clin Electrophysiol* 2011;34:1258–66.
- Barhaiya C, Po JK, Hanson S, et al. Tpeak-Tend and Tpeak-Tend/QT ratio as markers of ventricular arrhythmia risk in cardiac resynchronization therapy patients. *Pacing Clin Electrophysiol* 2013;36:193–8.
- Miyazaki F, Munetatsu Y, Ohnishi Y, et al. Increase in Tpeak-Tend interval induced by cardiac resynchronization therapy is a predictor of ventricular tachycardia. *J Arrhythmia* 2012;28:219–24.
- Nakai T, Tanabe J, Okabayashi H, et al. Development of a signal-averaged vector-projected 187-channel high-resolution electrocardiogram for the evaluation of the spatial location of high-frequency potentials and abnormal ventricular repolarization. *Int Heart J* 2007;48:701–13.
- Nakai T, Miyazaki F, Okabayashi H, et al. Newly developed signal-averaged vector-projected 187-channel electrocardiogram can evaluate the spatial distribution of repolarization heterogeneity. *Int Heart J* 2009;40:1513–64.

The new ECG telemedicine system using a smart phone; Comparison of Holter ECG

Hiroyuki Kamada¹⁾ Koichi Kurumatani²⁾ Takashi Hasegawa³⁾

¹⁾ Morioka Japanese Red Cross Hospital

²⁾ National Institute of Advanced Industrial Science and Technology

³⁾ Gunma University Hospital

Abstract: We have developed a new wireless ECG monitoring system (ABS-1) which transmits data via a Bluetooth-equipped smartphone. The quality of ABS-1 ECG was compared against the Holter ECG's in healthy volunteers. At the lowest heart rate of each individual, ABS-1 and Holter devices recorded identical waveforms of ECG. The results suggest that this new Bluetooth wireless ECG monitoring system can become a future compact and inexpensive ECG monitoring tool for health care management at home.

Keywords: ECG, Bluetooth, smartphone

要旨

スマートフォンに標準的に装備されている Bluetooth を使った心電計 (ABS-1) を開発した。この ABS-1 を使ったシステムから得られる心電図の品質を評価するために、ホルター心電計と ABS-1 を同時に装着して、その波形の比較を行った。本研究の結果、最小心拍数では両者の波形に違いは認められなかった。あたらしい心電図伝送システムは、小形で安価なシステムとして在宅医療や健康管理に活用されることが期待される。

イベントレコーダーと比較した特性について着目の文献的考察を行った。

2. 対象

健常ボランティア 6 名 (男性 3 名、女性 3 名、平均 52 ± 10 歳)

3. 方法

ホルター心電計 (テルモ社製 Holterc) と新しく開発した心電計 (ABS-1) のそれぞれの特性について【表 1】に示した。ホルター心電計と ABS-1 を同時に同一被験者に装着し、約 2 時間の心電図記録を行った。ホルター心電計は 2 誘導 (NAS4 と CM5)、ABS-1 は 1 誘導 (日本光電社製 デイスホ電機 T-50) を用いた【図 1】。ホルター心電計の心電図データは本体内のフラッシュメモリに記録され、検査終了後に専用機器 (行銀クレドール) に

1. はじめに

スマートフォンに標準的に装備される Bluetooth を使った通信機能をもつ小形心電計 (ABS-1) を開発した。本システムの臨床的有用性を検討する基礎データとしてホルター心電図検査の波形と心拍数トレンドグラフの相違の検討を行った。また従来から普及しているホルター心電図法

【表 1】ホルター心電計 (Holterc) と ABS-1 の仕様比較

	Holterc	ABS-1
誘導数	2 チャンネル	1 チャンネル
入力信号電圧範囲 (mV)	DC ± 150, AC ± 5	DC ± 6, AC ± 6
周波数特性 (Hz)	0.05 ~ 40	0 ~ 60
解像精度	10bit, 128Hz サンプリング	12bit, 200Hz サンプリング
記録媒体	32MB フラッシュメモリ	2GB フラッシュメモリ
通信方式	有線	無線 (Bluetooth)
記録時間	最長 25 時間	250 時間
満充電での連続稼働時間	不明 (25 時間保証)	9 時間
電源	ボタン電池リチウム電池 (CR2032) 1 個, DC3V	充電式リチウム電池, DC3.7V
サイズ、重さ (電池含む)	50 × 65 × 10	49 × 69 × 14
質量 (電池含む)	30g	25g
EMC 規格適合	IEC60951-1-2:1993 年	なし

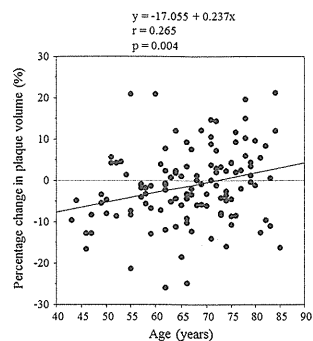
Table 3 Parameters evaluated using grayscale and virtual histology intravascular ultrasound

	Elderly (n = 72)			Non-elderly (n = 47)		
	Baseline	Follow-up	p value	Baseline	Follow-up	p value
EEM volume index (mm ³ /mm)	17.27 ± 5.49*	17.12 ± 5.55**	0.19	14.95 ± 4.71	14.52 ± 4.54	0.007
% change		-0.9 ± 5.1			-2.4 ± 6.3	
Plaque volume index (mm ³ /mm)	9.49 ± 3.63*	9.43 ± 3.52**	0.57	8.11 ± 2.56	7.80 ± 2.40	0.007
% change		0.0 ± 9.1*			-3.1 ± 8.9	
Lumen volume index (mm ³ /mm)	7.78 ± 2.53*	7.69 ± 2.63*	0.43	6.83 ± 2.63	6.72 ± 2.61	0.3
% change		-1.0 ± 12.5			-1.0 ± 10.5	
Percent atheroma volume (%)	54.5 ± 7.1	54.8 ± 7.0	0.58	54.7 ± 7.0	54.2 ± 7.0	0.35
Nominal change (%)		0.3 ± 4.5			-0.5 ± 3.6	
Fibrous volume index (mm ³ /mm)	3.49 ± 2.01	3.48 ± 1.83**	0.94	3.00 ± 1.48	2.61 ± 1.17	0.0004
Change (mm ³ /mm)		-0.01 ± 0.84*			-0.39 ± 0.70	
FF volume index (mm ³ /mm)	1.26 ± 1.10**	0.96 ± 0.77*	0.0006	0.79 ± 0.39	0.62 ± 0.63	0.1
Change (mm ³ /mm)		-0.30 ± 0.71			-0.17 ± 0.70	
NC volume index (mm ³ /mm)	0.75 ± 0.54	0.87 ± 0.56	0.06	0.73 ± 0.59	0.85 ± 0.63	0.1
Change (mm ³ /mm)		0.11 ± 0.50			0.15 ± 0.63	
DC volume index (mm ³ /mm)	0.47 ± 0.45	0.59 ± 0.54	0.002	0.38 ± 0.36	0.49 ± 0.44	0.01
Change (mm ³ /mm)		0.12 ± 0.32			0.11 ± 0.29	
Average length (mm)	25.7 ± 14.9			22.8 ± 15.0		

Data are expressed as mean ± SD

EEM external elastic membrane, FF fibro-fatty, NC necrotic-core, DC dense-calcium

* p < 0.05, ** p < 0.01 compared to non-elderly. #p = 0.07 compared to non-elderly

**Fig. 1** Correlation between age and percentage change in plaque volume during statin therapy. Age and percentage change in plaque volume during statin therapy showed a significant positive correlation**Table 4** Predictors of percentage change in plaque volume

	Univariate		Multivariate	
	r	p value	β	p value
Age	0.265	0.004	0.233	0.02
Gender	-0.127	0.17	0.012	0.9
Coronary artery disease status	-0.066	0.48		
Hypertension	0.163	0.08	0.063	0.53
Diabetes mellitus	0.137	0.14	0.06	0.54
Smoking	0.088	0.34		
eGFR	-0.035	0.71		
Type of statin	-0.074	0.43		
Percentage change in LDL-C	-0.001	0.99		
Percentage change in sd-LDL	-0.097	0.34		
Percentage change in HDL-C	-0.114	0.22		
Percentage change in hs-CRP	0.056	0.56		
Change in EPA + DHA/AA	-0.24	0.02	-0.209	0.04

Male gender, unstable angina pectoris, hypertension, diabetes mellitus, smoking, and pitavastatin use were assigned a value of 1. Female gender, stable angina pectoris, normal blood pressure, absence of diabetes and smoking, and pravastatin use were assigned a value of 0. eGFR estimated glomerular filtration rate, LDL-C low-density lipoprotein cholesterol, hs-CRP high-sensitivity C-reactive protein, EPA eicosapentaenoic acid, DHA docosahexaenoic acid, AA arachidonic acid

Springer

the percentage change in plaque volume was different between the elderly and non-elderly patients. Furthermore, age showed a significant positive correlation with the percentage change in plaque volume and a significant predictor associated with the percentage change in plaque volume during statin therapy.

Glavog et al. [12] described vascular remodeling as a compensatory enlargement of the coronary artery in response to an increase in plaque area. In histological studies, expansion in vessel size is associated with an increase in inflammatory cells and proteolytic enzymes [13, 14]. In clinical IVUS studies, expansive remodeling is associated with plaque instability and unstable clinical presentation [15–17]. Consistent with previous findings from human autopsies [2] and IVUS [3–5, 18], our results demonstrated that coronary atherosclerosis was more advanced with expanding remodeling and greater atheroma volume in the elderly patients. Furthermore, a significant negative vessel remodeling and regression in plaque volume during statin therapy were observed only in the non-elderly patients. Thus, atherosclerosis accelerated with age [1], even in patients who received statin therapy.

According to VH-IVUS, the fibro-fatty plaque component is associated with development of acute coronary syndrome [19]. As reported in the main TRUTH trial [8], a decrease in the fibro-fatty plaque component and an increase in the calcified component were observed in both the elderly and non-elderly patients. Consistent with previous studies [20, 21], statins induced significant changes in the composition of coronary atherosclerosis without a significant regression in coronary artery plaques in the elderly patients, which illustrated the potential effects of statin against coronary events even in these high risk patients with elderly. Statin therapy reduces matrix metalloproteinase activity, apoptosis, and macrophages, and increases collagen content [22]. These changes could explain the qualitative changes observed in coronary artery plaque composition without a regression in plaque volume. However, a large amount of atheroma volume, particularly the fibro-fatty plaque component, before and during statin therapy may affect the development of coronary events in the elderly patients. As several studies have reported that statins have no effect on necrotic-core accumulation [8, 23, 24], statin therapy could not halt the progression of the necrotic-core component in this study.

Current lipid-lowering guidelines focus on LDL-C reduction as a principal target for primary and secondary prevention of cardiovascular disease [25]. Indeed, clinical trials using statins have demonstrated reductions in cardiovascular events and atheroma progression [6–8, 26]. However, not only serum LDL-C but also serum HDL-C, the LDL-C/HDL-C ratio, and other parameters are useful markers of atheroma regression and/or inhibition of

progression in coronary artery plaques [27–29]. Recently, we reported that >40 % of patients receiving statin therapy continued to demonstrate atheroma progression [30]. Thus, not all patients show reductions in cardiovascular events and regression in coronary atherosclerosis under statin therapy. Bayturan et al. [31] reported that residual risk factors associated with atheroma progression in patients who achieve very low LDL-C levels (<70 mg/dl) included baseline percent atheroma volume, presence of diabetes mellitus, increase in systolic blood pressure, less increase in HDL-C, and a smaller decrease in apolipoprotein B levels. This suggests the need for intensive control of global atherosclerotic risk factors to produce regression in coronary atherosclerosis. However, although serum LDL-C, apolipoprotein B, and sd-LDL levels were significantly lower in the elderly patients, a significant regression in plaque volume was observed only in the non-elderly patients. Considering change in the EPA + DHA/AA ratio was a significant predictor of the percentage change in plaque volume, the residual risk for cardiovascular events during statin therapy can be explained in part by n-3 to n-6 polyunsaturated fatty acids ratios [32]. More recently, Puri et al. [33] reported that greater baseline atheroma volume was associated with less disease progression while older age was a significant predictor of atheroma progression with potent statin therapy. Although coronary atherosclerosis was more advanced in the elderly patients, statin-induced regression in plaque volume and negative vessel remodeling were attenuated. This suggests that atheroma regression in older individuals in general may be more difficult to achieve.

A meta-analysis demonstrated that effects of statin on major vascular events were similar among patients with age <65, >65 to <75, >75 years [34]. However, a large-scale, prospective, uncontrolled study performed in Japan reported that incidence of cardiovascular events during statin therapy was highest in patients aged >65 years old in the secondary prevention cohort [35]. Therefore, statin therapy may have less impact on the secondary prevention in Japanese patients with elderly.

Study limitations

The present study had several limitations. First, it is a post hoc subanalysis of the TRUTH trial. Second, although we excluded patients with angiographically apparent thrombi, an intraluminal thrombus might have influenced the study results. Third, IVUS examinations were performed only in the culprit vessel. Mechanical interventions might have affected the atheroma measurements because target segment of interest was located in the proximal site of culprit lesion in some patients and maximum necrotic-core area

Springer

has been often located proximal of the most severe stenosis site [36]. Finally, the small number of patients meant that the study's statistical power was insufficient to evaluate differences between the elderly and non-elderly patients. Therefore, a prospective multicenter study involving more patients is required to confirm our conclusions.

Conclusions

Coronary atherosclerosis was more advanced and vascular responses to statin therapy were attenuated in the elderly patients compared to the non-elderly patients.

Conflicts of interest None.

References

- Lakatta EG, Levy D (2003) Arterial and cardiac aging: major shareholders in cardiovascular disease enterprises: part I: aging arteries: a "set up" for vascular disease. *Circulation* 107:139–146
- Burke AP, Farb A, Pestaner J, Malcom GT, Zieske A, Kutys R, Smailke J, Virmani R (2002) Traditional risk factors and the incidence of sudden coronary death with and without coronary thrombosis in blacks. *Circulation* 105:419–424
- Hong YJ, Jeong MH, Ahn Y, Sim DS, Chung JW, Cho JS, Yoon NS, Yoon HJ, Moon JY, Kim KH, Park HW, Kim JH, Cho JG, Park JC, Kang JC (2008) Age-related differences in intravascular ultrasound findings in 1,009 coronary artery disease patients. *Circ J* 72:1270–1275
- Ruiz-Garcia J, Lerman A, Weisz G, Mochales A, Mintz GS, Fahy M, Xu K, Lantsky AJ, Cristea E, Farah TG, Teles R, Bolker HE, Templin B, Zhang Z, Aronson E, Farah TG, Teles R, Bolker HE, Templin B, Zhang Z, Aronson E, Farah TG, Teles R, Bolker HE (2012) Age- and gender-related changes in plaque composition in patients with acute coronary syndrome: the prospective study. *Euro Interv* 8:929–938
- Qian J, Mochales A, Mintz GS, Margolis MP, Lerman A, Rogers J, Banaei S, Kazzabi S, Castellanos C, Dani L, Fahy M, Stone GW, Leon MB (2009) Impact of gender and age on in vivo intravascular ultrasound-intravascular ultrasound imaging plaque characterization from the global Virtual Histology Intravascular Ultrasound (VH-IVUS) registry. *Am J Cardiol* 103:1210–1214
- Nissen SE, Tuzcu EM, Schoenhagen P, Brown BG, Ganz P, Vogel RA, Crowe T, Howard G, Cooper CJ, Brodie B, Grines CL, DeMaio AN, REVERSAL Investigators (2004) Effect of intensive compared with moderate lipid-lowering therapy on progression of coronary atherosclerosis: a randomized controlled trial. *JAMA* 291:1071–1080
- Nissen SE, Nicholls SJ, Sipahi I, Libby P, Raichlen JS, Ballantyne CM, Davignon J, Erbel R, Fruchart JC, Tarfiri J, Schoenhagen P, Crowe T, Cain V, Wolski K, Goormastic M, Tuzcu EM, ASTEROID Investigators (2006) Effect of very high-intensity statin therapy on regression of coronary atherosclerosis: the asteroid trial. *JAMA* 295:1556–1565
- Nozue T, Yamamoto S, Tohyama S, Umezawa S, Kunishima T, Sato A, Miyake S, Takeyama Y, Morino Y, Yamachi T, Muramatsu T, Hibi K, Soza T, Michishita I (2012) Statin Treatment for coronary artery plaque composition based on intravascular ultrasound radiofrequency data analysis. *Am Heart J* 163:191–199

- Nozue T, Yamamoto S, Tohyama S, Umezawa S, Kunishima T, Sato A, Miyake S, Takeyama Y, Morino Y, Yamachi T, Muramatsu T, Hibi K, Soza T, Michishita I; Kanagawa PTCA Conference Study Group (2009) Treatment with statin on atheroma regression evaluated by intravascular ultrasound with virtual histology (TRUTH study): rationale and design. *Circ J* 73:352–355
- Garcia-Garcia HM, Mintz GS, Lerman A, Vince DG, Margolis MP, van Es GA, Morel MA, Nair A, Virmani R, Burke AP, Stone GW, Serruys PW (2009) Tissue characterization using intravascular radiofrequency data analysis: recommendations for acquisition, analysis, interpretation and reporting. *Euro Interv* 5:177–189
- Mintz GS, Nissen SE, Anderson WD, Bailey SR, Erbel R, Fitzgerald PJ, Pinto FJ, Rosenfield K, Siegel RJ, Tuzcu EM, Yock PG (2001) American college of cardiology clinical expert consensus document on standards for acquisition, measurement and reporting of intravascular ultrasound studies (IVUS): a report of the American College of Cardiology Task Force on Clinical Expert Consensus Documents. *J Am Coll Cardiol* 37:1478–1492
- Glavog S, Weisenberg E, Zarins CK, Stankovic S, Koletis GJ (1987) Compensatory enlargement of human atherosclerotic coronary arteries. *N Engl J Med* 316:1371–1375
- Burke AP, Kolodgie FD, Farb A, Weber D, Virmani R (2002) Morphological predictors of arterial remodeling in coronary atherosclerosis. *Circulation* 105:297–303
- Yamamoto S, Mihls PG, Davies MJ (2002) Relationship between coronary artery remodeling and plaque vulnerability. *Circulation* 105:939–943
- Fujita K, Carlier SG, Mintz GS, Wijns W, Colombo A, Bose D, Erbel R, de Ribamar Costa J Jr, Kimura M, Sano K, Costa RA, Lui J, Stone GW, Moses JW, Leon MB (2005) Association of plaque characterization by intravascular ultrasound virtual histology and arterial remodeling. *Am J Cardiol* 96:1476–1483
- Nakamura M, Nishikawa H, Mukai S, Setsuba M, Nakajima K, Tamada H, Suzuki H, Ohnishi T, Kakuta Y, Nakano T, Yeung AC (2001) Impact of coronary artery remodeling on clinical presentation of coronary artery disease: an intravascular ultrasound study. *J Am Coll Cardiol* 37:63–69
- Schoenhagen P, Ziada KM, Kapadia SR, Crowe TD, Nissen SE, Tuzcu EM (2000) Extent and direction of artery remodeling in stable versus acute coronary syndromes: the intravascular ultrasound study. *Circulation* 101:598–603
- Ehara S, Naruko T, Kobayashi Y, Kataoka T, Nakagawa M, Shirai N, Ishii H, Okuyama T, Oe H, Sugioaka K, Hozumi T, Haze K, Yoshikawa J, Yoshiyama M, Ueda M (2007) Comparison of clinical characteristics and arterial remodeling by intravascular ultrasound imaging in three age groups (< or = 55, 56–69 and > or = 70 years) of Japanese patients with acute myocardial infarction. *Am J Cardiol* 100:1713–1717
- Sumrelli JF, Nasu K, Fujita H, Terashima M, Matsubara T, Tsuchikane E, Ehara M, Kinoshita Y, Zheng QX, Tanaka N, Katoh O, Suzuki T (2006) Coronary plaque composition of culprit-rupture lesions according to the clinical presentation: a virtual histology intravascular ultrasound analysis. *Eur Heart J* 27:2939–2944
- Kawasaki M, Sano K, Okubo M, Yokoyama H, Ito Y, Murata I, Tsuchiya K, Minatoguchi S, Zhou X, Fujita H, Fujiwara H (2005) Volumetric quantitative analysis of tissue characteristics of coronary plaques after statin therapy using three-dimensional integrated backscatter intravascular ultrasound. *J Am Coll Cardiol* 45:1946–1953
- Scharf M, Bocksch W, Koschik DH, Voelker W, Karsch KR, Kreuzer J, Hausmann D, Beckmann S, Grosse M (2001) Use of intravascular ultrasound to compare effects of different strategies of lipid-lowering therapy on plaque volume and composition in patients with coronary artery disease. *Circulation* 104:387–392

Springer

Springer

Zhi Yang Ng, MBBS
Department of Orthopaedic Surgery
Alexandra Hospital, Singapore

Alphonsus Khin Sze Chong, FAMS (Hand Surgery)
Department of Hand and Reconstructive
Microsurgery

National University Hospital, Singapore

Yong Loo Lin School of Medicine

National University of Singapore, Singapore

<http://dx.doi.org/10.1016/j.jhsa.2012.11.004>

Gouty Tophus of the Second Metacarpal Simulating a Malignancy With Pathologic Fracture

To the Editor:

We report on an intraosseous gouty tophus in the second metacarpal causing a pathologic fracture and simulating a malignancy.

A 5-year-old girl with a swollen hand was referred with a diagnosis of a bone tumor. She had been treated for hypoplastic left heart syndrome with protein-loosening enteropathy. She has had 5 surgical interventions, including a fenestrated Fontan procedure. She took many medications, including enalapril maleate. She had generalized edema, hepatosplenomegaly, and ascites. A 2 × 2 cm mass was palpable over the second metacarpal. Slight redness, local heat, and swelling without tenderness were noted. The blood urea nitrogen and uric acid levels were 75.5 mg/dL and 19.1 mg/dL, respectively, much higher than usual, whereas the creatinine level was normal, 0.7mg/dL. Total protein was 4.4 g/dL; albumin was 2.8 g/dL; and immunoglobulins were IgG, 128mg/dL; IgA, 30mg/dL and IgM, 56mg/dL, lower than usual. Radiographs showed an ill-margined lytic and sclerotic lesion with a pathologic fracture and periosteal reaction (Fig. 1). Magnetic resonance imaging showed a low-signal-intensity mass on T1-WI and marked high signal intensity on T2-WI surrounding the metacarpus. A needle biopsy was performed. The birefringent crystals suggesting gouty tophus were seen without distinctive inflammatory cellular infiltration histologically. Because of progressively deteriorating renal function, the enalapril maleate was discontinued. Consequently, her renal dysfunction improved, and the uric acid level decreased to 6.4mg/dL. The gouty tophus decreased in size.

The authors thank Dr. Gamaliel Tan Yu Heng for permission to proceed with the study.

REFERENCES

- Cockshott WP. Carpal fusions. *Am J Roentgenol Radium Ther Nucl Med.* 1963;89(1):1260-1271.
- Minaar AB. Congenital fusion of the lunate and triquetral bones in the South African Bantu. *J Bone Joint Surg Br.* 1952;34(1):45-48.
- Weinzwilg J, Providence RI, Kirk Watson H, Shaer JA. Congenital synchondrosis of the scaphotrapezio-trapezoidal joint. *J Hand Surg Am.* 1997;22(1):74-77.



FIGURE 1: Posteroanterior x-ray of the left hand showing a poorly marginated lytic and sclerotic lesion in the second metacarpal associated with periosteal reaction and a pathological fracture.

Enalapril maleate might have caused hyperuricemia and the gouty tophus, which was painless. Hypo-globulinemia might have been responsible for the patient's lack of pain. The immunoglobulin G was strongly absorbed from serum to monosodium urate

JHS • Vol 38A, January 2013

LETTERS TO THE EDITOR

289

crystals in gouty tophi.¹ Histological findings did not reveal inflammatory cellular infiltration.

Gouty tophus should be included in the differential diagnosis of the patient considered to have a bone tumor in the hand.

Yukinori Yaegashi, MD

Jun Nishida, MD

Department of Orthopaedic Surgery
Iwate Medical University
Morioka, Japan

Kotaro Oyama, MD

Department of Pediatric Cardiology

Iwate Medical University Memorial Heart Center

Morioka, Japan

<http://dx.doi.org/10.1016/j.jhsa.2012.10.044>

REFERENCE

- Hasselbacher P, Schumacher HR. Immunoglobulin in tophi and on the surface of monosodium urate crystals. *Arthritis Rheum.* 1978;21(3):353-361.

Letter Regarding "Perilunate Dislocations and Fracture Dislocations"

To the Editor:

We read with great interest the article by Jones and Kakar.¹ It nicely covers the whole spectrum of perilunate dislocations and fracture dislocations. The author did not mention the treatment for dislocations in patients who present late. The treatment mentioned is about the salvage procedure directly. It is mentioned in the literature that open reduction internal fixation in a single stage² as well as in a 2-staged procedure³ is a satisfactory procedure if executed properly in patients who present late. The results of these procedures have been satisfactory.⁴ Proximal row carpectomy or wrist arthodesis might not be acceptable to young patients. Because this injury pattern is mainly seen in young individuals, the option of 2-stage reduction should be given to patients. If this method fails, only then should we proceed to a salvage procedure.

Mohammed Tahir Ansari, MBBS, MS
Department of Emergency Medicine
All India Institute of Medical Sciences
New Delhi, India

Prakash P. Kotwal, MBBS, MS
Department of Orthopaedics
All India Institute of Medical Sciences
New Delhi, India

<http://dx.doi.org/10.1016/j.jhsa.2012.10.047>

REFERENCES

- Jones DB Jr, Kakar S. Perilunate dislocations and fracture dislocations. *J Hand Surg Am.* 2012;37(10):2168-2174.
- Kaifu L, Zhou X, Fuguo H. Chronic perilunate dislocations treated with open reduction and internal fixation: results of medium-term follow-up. *Int Orthop.* 2010;34(8):1315-1320.
- Lal H, Jangfja V, Kakran R, Mittal D. Two stage procedure for neglected transscaphoid perilunate dislocation. *Indian J Orthop.* 2012; 46(3):351-355.

- Gang B, Goyal T, Kotwal PP. Staged reduction of neglected transscaphoid perilunate fracture dislocation: A report of 16 cases. *J Orthop Surg Res.* 2012;7:19.

In Reply:

We thank the reader for the insightful comments and for highlighting several papers¹⁻³ (2 of which were published after our manuscript was submitted) addressing the particularly challenging subset of perilunate injuries presenting to the hand surgeon late. Massoud and Naam also recently reported their experience with open reduction internal fixation of perilunate dislocations and fracture dislocations that were treated 13 to 35 weeks from the time of injury, with good to excellent results in 11 of 19 patients.⁴ Although these studies represent relatively small series, they do demonstrate that successful outcomes can be achieved with single-stage or double-stage open reduction internal fixation procedures in the treatment of chronic perilunate injuries. However, the carpus should be easily reducible at the time of surgery, or any form of ligamentous repair can be prone to failure with time. Although these series have not demonstrated loss of intercarpal reduction over time, repair of the intercarpal ligaments can prove challenging secondary to their attenuation and contracture related to the chronicity of the injury. In addition, the articular cartilage must be evaluated at the time of surgery. Kailu et al noted, "With no exception, cases with excellent or good results in this study had satisfactory cartilage condition of the midcarpal joints when evaluated during the operation," and 2 patients with poor outcomes had been noted to have severe scaphoid and lunate cartilage contusion at the time of open reduction.¹ Therefore, in the setting of severe chondral injury, arthritis, or avascular necrosis associated with a

JHS • Vol 38A, January 2013

Genetic Background of Catecholaminergic Polymorphic Ventricular Tachycardia in Japan

Mihoko Kawamura, MD; Seiko Ohno, MD, PhD; Nobu Naiki, MD; Iori Nagaoka, MD, PhD; Kenichi Dochi, MD; Qi Wang, BSc; Kanae Hasegawa, MD; Hiromi Kimura, MD, PhD; Akashi Miyamoto, MD, PhD; Yuka Mizusawa, MD, PhD; Hideki Itoh, MD, PhD; Takeru Makiyama, MD, PhD; Naokata Sumitomo, MD, PhD; Hiroya Ushinohama, MD; Kotaro Oyama, MD, PhD; Nobuyuki Murakoshi, MD, PhD; Kazutaka Aonuma, MD, PhD; Hitoshi Horigome, MD, PhD; Takafumi Honda, MD, PhD; Masao Yoshinaga, MD, PhD; Makoto Ito, MD, PhD; Minoru Horie, MD, PhD

Background: The genetic background of catecholaminergic polymorphic ventricular tachycardia (CPVT) has been extensively investigated for the last decade in Western countries, but it remains unstudied in the Asian population.

Methods and Results: In 50 Japanese probands from unrelated families who satisfied clinical criteria for CPVT, genetic testing was conducted in all exons on 3 CPVT-related genes: cardiac ryanodine receptor 2 (RYR2), calstretin 2 (CASQ2) and inward rectifier potassium channel 2 (KCNJ2), and the clinical features between RYR2-genotyped and -non-genotyped patient groups were compared. Genetic and clinical evaluation was also done in 46 family members. In the genetic screening, 28 (18 novel) RYR2 (56.0%), 1 compound heterozygous CASQ2 (2.0%) and 1 KCNJ2 (2.0%) mutation carriers were identified. In the RYR2 mutation-positive group, the frequency of bidirectional ventricular tachycardia and the use of beta-blockers were significantly higher than in the mutation-negative group. In contrast, there was no significant difference in supraventricular arrhythmias between the 2 groups. With regard to disease penetrance, the number of family members of RYR2-genotyped probands with a clinical diagnosis of CPVT was high.

Conclusions: Thirty gene mutation carriers were found for 3 genes in 50 probands clinically diagnosed as having CPVT. The penetrance of CPVT phenotype was significantly higher in RYR2 mutation carriers, thus RYR2 gene screening in CPVT patients would be indispensable to prevent unexpected cardiac sudden death of young family members. (Circ J 2013; 77: 1705-1713)

Key Words: Beta-blockers; Calstretin; Catecholaminergic polymorphic ventricular tachycardia; Flecainide; Ryanodine receptor

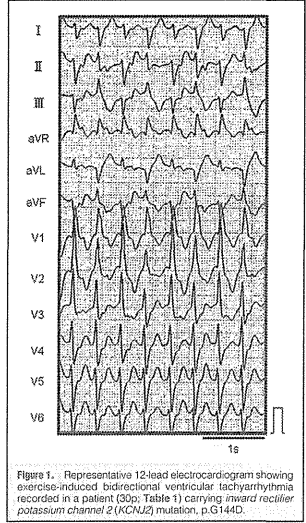


Figure 1. Representative 12-lead electrocardiogram showing exercise-induced bidirectional ventricular tachycardia recorded in a patient (30p; Table 1) carrying inward rectifier potassium channel 2 (KCNJ2) mutation, p.G144D.

tions were identified in a gene encoding a cardiac ryanodine receptor (RYR2; MIM 189002).^{5,6-10} Homozygous or compound heterozygous mutations in calstretin 2 (CASQ2; MIM 114251) were then reported to cause the second variant of CPVT (CPVT2).¹¹⁻¹³ CASQ2 encodes a Ca-binding protein in the sarcoplasmic reticulum and plays a key role in maintaining cytosolic Ca²⁺ concentration, in collaboration with RYR2. In 2009, the third variant of CPVT was reported to result from a mutation in KCNJ2 (MIM 600681), which encodes Kir2.1, a subunit for inward-rectifier potassium channels.¹⁴ The KCNJ2 mutation (p.V227F) produced no functional defects on Kir2.1 channels at rest but an unusual latent loss of function regarding the cAMP-dependent protein kinase A (PKA)-dependent phosphorylation of Kir2.1 channel proteins.¹⁴ This in turn leads to the loss of response to beta-adrenergic stimulation. More recently, Bhuiyan et al reported a new malignant variant of CPVT in an inbred family with autosomal recessive inheritance. They have mapped this recessive CPVT locus to chromosome 7p14-p22.¹⁵ Koushi-Bakson et al identified triadin (TRDN) as a new gene responsible for an autosomal recessive form of CPVT.¹⁶

To date, there are a substantial number of reports on the genetic background in CPVT cohorts from Western countries,^{2,4,6-11,13,15,16} but few in Asian populations.¹⁷⁻²¹ In the present study, we therefore conducted genetic testing on 3 CPVT-related candidate genes - RYR2, CASQ2, and KCNJ2 - in 50 CPVT probands from unrelated Japanese families and their 46 family members and examined their correlation with clinical phenotypes.

Methods

Subjects: Fifty clinically diagnosed CPVT probands and their 46 family members (total, 96) were included in genetic analysis. The entry criteria were the presence of the following arrhythmias documented on exercise stress testing and/or Holter monitoring electrocardiogram (ECG) in the absence of structural heart abnormalities: bVT (Figure 1); pVT; or ventricular fibrillation (VF). The characteristic QRS morphology of bVT or pVT is a change in QRS axis every other beat, with 2 or more types of patterns, during more than 4 consecutive beats. We also included a 2-year-old boy without typical arrhythmias but whose father was symptomatic and genetically diagnosed as CPVT and who died suddenly in his 30s (Table 1; 13-p). We excluded patients who suffered bVT or pVT due to prominent electrolyte imbalance, drug treatment, or organic heart disease such as cardiomyopathy, ischemic heart disease, or congenital heart disease. Primary electrical diseases such as long QT syndrome (LQTS) were also excluded. Bradycardia was defined as follows: in children aged <16 years, heart rate below the second percentile of established age- and sex-appropriate norms;²² in adults, <60 beats/min on resting ECG without intake of beta-blocker.

Mutation Analysis

The protocol for genetic analysis was approved by the Institutional Ethics Committee and was performed under its guidance. All subjects gave written informed consent before genetic analysis. Genomic DNA was isolated from peripheral white blood cells. Intron primers amplifying the RYR2, CASQ2 and KCNJ2 coding regions were used for polymerase chain reaction (PCR) amplifications as previously reported.^{5,7,10,13,23} PCR products were analyzed on direct sequencing. The cDNA sequences of RYR2, CASQ2 and KCNJ2 were based on the GenBank reference sequence NM_001035.2, NM_001232.3 and NM_000891.2, respectively. Regarding RYR2 mutation-negative probands, we also searched for large genomic rearrangements affecting exon 3 and 97, as reported previously.⁴ In addition to these 3 genes, we examined the entire coding sequence for KCNQ1, KCNH2, SCN5A, and KCNE1-5 to exclude an unexpected presence of compound mutations related to primary electrical diseases.

All novel putative pathogenic variants were examined and confirmed to be absent in 400 chromosomes from 200 Japanese controls.

Statistical Analysis

All continuous variables are reported as mean±SD. Differences between continuous variables were evaluated using unpaired Student's t-test, and categorical variables using chi-squared analysis. Statistical significance was set at P<0.05.

Results

Genetic Analysis (CPVT1) The genetic analysis for RYR2 identified 26 different missense heterozygous mutation carriers and 2 carriers with large DNA deletions including exon 3 in 50 probands.

Catecholaminergic polymorphic ventricular tachycardia (CPVT) is a form of inherited cardiac arrhythmia, characterized by polymorphic or bidirectional ventricular tachycardia (pVT or bVT) induced by physical exercise, emotional stress or catecholamine use.¹⁻³ CPVT patients have autosomal dominant or recessive traits. The QTc interval is generally within the normal range, but sinus bradycardia and atrial arrhythmias have been associated with CPVT.¹⁻²

Editorial p1684

The first gene locus mapped to chromosome 1q42-43* was an autosomal dominant form of CPVT (CPVT1), and mutations were identified in a gene encoding a cardiac ryanodine receptor (RYR2; MIM 189002).^{5,6-10} Homozygous or compound heterozygous mutations in calstretin 2 (CASQ2; MIM 114251) were then reported to cause the second variant of CPVT (CPVT2).¹¹⁻¹³ CASQ2 encodes a Ca-binding protein in the sarcoplasmic reticulum and plays a key role in maintaining cytosolic Ca²⁺ concentration, in collaboration with RYR2. In 2009, the third variant of CPVT was reported to result from a mutation in KCNJ2 (MIM 600681), which encodes Kir2.1, a subunit for inward-rectifier potassium channels.¹⁴ The KCNJ2 mutation (p.V227F) produced no functional defects on Kir2.1 channels at rest but an unusual latent loss of function regarding the cAMP-dependent protein kinase A (PKA)-dependent phosphorylation of Kir2.1 channel proteins.¹⁴ This in turn leads to the loss of response to beta-adrenergic stimulation. More recently, Bhuiyan et al reported a new malignant variant of CPVT in an inbred family with autosomal recessive inheritance. They have mapped this recessive CPVT locus to chromosome 7p14-p22.¹⁵ Koushi-Bakson et al identified triadin (TRDN) as a new gene responsible for an autosomal recessive form of CPVT.¹⁶

Received November 27, 2012; revised manuscript received January 30, 2013; accepted February 26, 2013; released online April 18, 2013. Time for primary review: 20 days. Department of Cardiovascular and Respiratory Medicine, Shiga University of Medical Science, Otsu (M.K., S.O., N.N., I.N., K.D., Q.W., K.H., H.K., A.M., Y.M., H.L., M.I., M.H.); Department of Cardiovascular Medicine, Kyoto University Graduate School of Medicine, Kyoto (T.M.); Department of Pediatrics and Child Health, Nihon University School of Medicine, Tokyo (N.S.); Department of Pediatric Cardiology, Fukuoka Children's Hospital and Medical Center for Infectious Disease, Fukuoka (H.U.); Department of Pediatric Cardiology, Iwate Medical University Memorial Heart Center, Morioka (K.O.); Cardiovascular Division, Graduate School of Comprehensive Human Sciences, University of Tsukuba, Tsukuba (N.M., K.A.); Department of Pediatrics, Tsukuba University Hospital, Tsukuba (H.H.); Department of Pediatrics, Tokyo Women's Medical University Yachyo Medical Center, Tokyo (T.H.); and Department of Pediatrics, National Hospital Organization Kagoshima Medical Center, Kagoshima (M.Y.), Japan. Mailing address: Minoru Horie, MD, PhD, Department of Cardiovascular and Respiratory Medicine, Shiga University of Medical Science, Seta-Tsukinowa, Otsu 520-2192, Japan. E-mail: horie@belle.shiga-med.ac.jp ISSN-1346-9843 doi:10.1253/circ.CJ-12-1460 All rights are reserved to the Japanese Circulation Society. For permissions, please e-mail: cj@j-circ.or.jp

Genetic Background in CPVT

Table 1. Characteristics of Genetic Mutation Carriers in CPVT Patients. Columns include Family number, Proband number, Sex, Age at onset, Exercise related syncope, Required CPR, HR at rest, QTc, bVT, pVT, VF, Atrial tachyarrhythmias, Other arrhythmias, beta-blockers, and Dosage of beta-blockers.

(Table 1 continued the next page.)

Table 2. Mutation details for various probands. Columns include Other medicine, ICD, Gene, Exon, Nucleotide change, Protein change, Previous report, Exercise stress test, Pharmacologic stress test, Sudden death, and Diagnosed CPVT.

Age at onset, age at which patients experienced the first symptomatic arrhythmic attack or were recorded as having physical stress-induced ventricular tachycardia. *NM_001035.2; **NM_001232.3; ***NM_000891.2. AF, atrial fibrillation; AFI, atrial flutter; AT, atrial tachycardia; bVT, bidirectional ventricular tachycardia; CASQ2, calstretin 2; CPCR, cardiac pacemaker; calsequestrin 2; CPVT, catecholaminergic polymorphic ventricular tachycardia; HR, heart rate; ICD, implantable cardioverter-defibrillator; KCNJ2, inward rectifier potassium channel 2; NA, not available; PM, pacemaker; PVC, premature ventricular contraction; pVT, polymorphic ventricular tachycardia; QTc, corrected QT interval; RYR2, cardiac ryanodine receptor; VF, ventricular fibrillation.